Distinct modes of endocytotic presynaptic membrane and protein retrieval at the calyx of Held terminal

Yuji Okamoto

Graduate School of Brain Science, Doshisha University

A thesis submitted for the degree of

Doctor of Philosophy in Science

March 2018

Abstract

Neurotransmitter is released at synapses by fusion of synaptic vesicles with the plasma membrane. To sustain synaptic transmission, membranes and vesicular proteins has to be retrieved for reuse. I have combined capacitance measurements and pH-imaging via a pH-sensitive vesicular protein marker (anti-synaptotagmin2-cypHer5E), and compared the retrieval kinetics of membranes and synaptotagmin2 (Syt2) at the calyx of Held presynaptic terminal. Membrane and Syt2 were retrieved with a similar time course as slow endocytosis was elicited, suggesting that both were retrieved simultaneously by relatively small vesicles. When fast endocytosis was elicited with massive stimulation, Syt2 was still retrieved together with the membrane, but re-acidification of endocytosed organelles was slowed down, which suggests that massive stimulation caused bulk endocytosis of large vesicles. Calmodulin (CaM) inhibitors or the inhibition of the Ca^{2+}-CaM-Munc13-1 signaling pathway only impaired the retrieval of Syt2 while leaving membrane retrieval intact. This indicates that Ca^{2+}-CaM regulates the retrieval of Syt2, and that Munc13-1 is a possible downstream target of CaM. This data identifies a novel mechanism of stimulus- and Ca^{2+}-dependent regulation of coordinated endocytosis of synaptic membranes and Syt2.

Acknowledgements

I would like to thank my supervisors, Dr. Takeshi Sakaba and Dr. Mitsuharu Midorikawa, for their continuous guidance, scientific advice, and encouragement during last 5 years. I would also like to thank Dr. Shin-ya Kawaguchi for his insightful comments.

I would like to express my gratitude to Dr. Noa Lipstein, Dr. Nils Brose, Dr. Yungfeng Hua, Dr. Kun-Han Lin and Ina Herfort. This study would not have been completed without their technical assistance.

I also expand my gratitude to Dr. Shigeo Takamori, Dr. Hiroaki Misono and Dr. Nobuyuki Nukina for being my thesis committee members despite of their busy schedule.

I am grateful to the Doshisha University scholarship for doctoral students and the JSPS predoctoral fellowship for financial support.

I am also profoundly grateful to the past and the present members in the Sakaba lab, colleagues in Doshisha and my friends for all the good times. A special thanks to my family for everything.

Table of Contents

Abbreviations

AP	action potential
AP-2	adaptor protein 2
AP180	adaptor protein 180
AZ	active zone
CaM	calmodulin
CAST	cytomatrix at the active zone (CAZ)-associated structural protein
C_m	membrane capacitance
GFP	green fluorescent protein
I_{Ca}	calcium current
KI	knock-in
Munc13-1^{W464R}	a point mutation in exon 11 of the *Unc13a* gene replaces the tryptophan in position 464 of Munc13-1 by an arginine
peri-AZ	peri-active zone
RIM	Rab3 interacting molecule
ROI	region of interest
RRP	readily releasable pool
SNAP-25	synaptosomal-associated protein 25
SNARE	soluble N-ethylmaleimide-sensitive factor (NSF) attachment protein receptor
SV	synaptic vesicle
SV2	synaptic vesicle protein 2
Syt1/2	synaptotagmin 1/2
TTX	tetrodotoxin
TEA	tetraethylammonium
VAMP2	vesicle-associated membrane protein 2
V-ATPase	vacuolar-type H^+-ATPase
VGLUT	vesicular glutamate transporter
V_m	membrane potential
WT	wild type
τ	time constant

1. Introduction

Neurons are independent elements, that communicate with each other at intercellular junctions called synapses. Synapses are classified into electrical synapses and chemical synapses. Electrical synapses transmit electrical signals directly from one neuron to another through specialized channels called gap junctions, which physically connect between pre- and postsynaptic neurons. In contrast, chemical synapses use chemical compounds called neurotransmitters to transmit signals from one neuron to another cell, usually neurons or muscle cells.

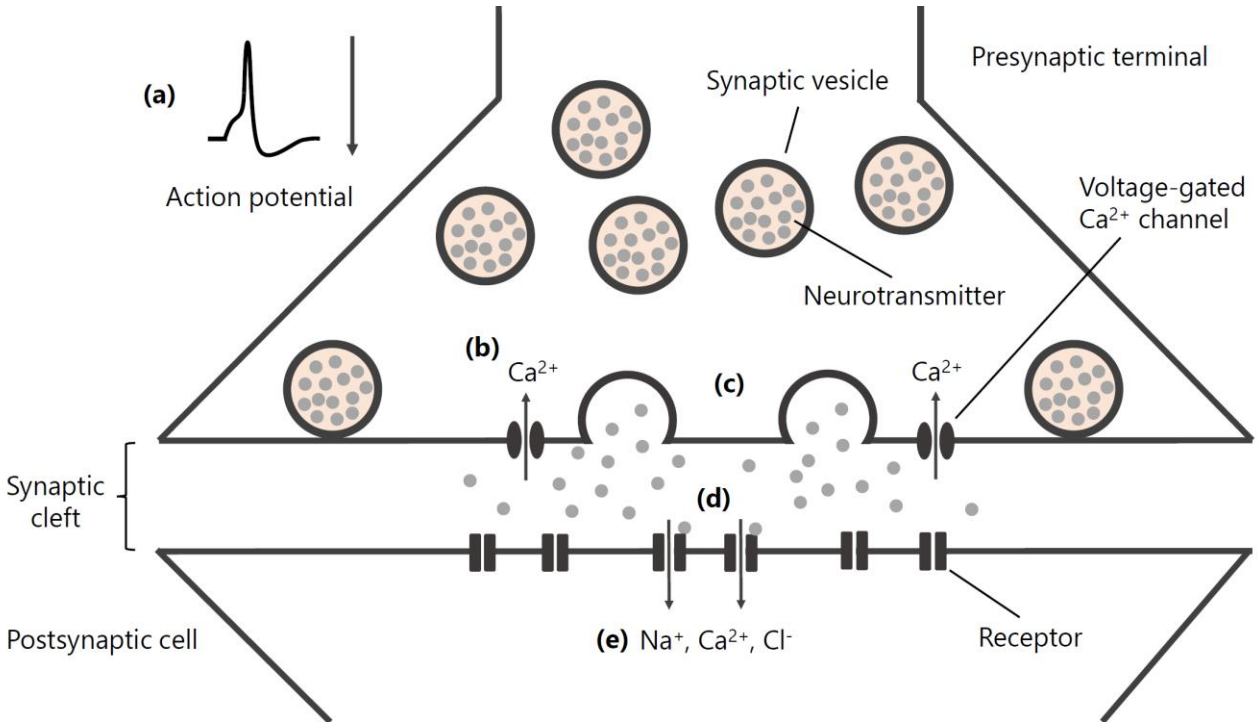

Figure 1. Schematic view of synaptic transmission

Chemical synapses are composed of a presynaptic terminal, synaptic cleft and a postsynaptic cell. At the presynaptic terminal, neurotransmitters are stored inside synaptic vesicles (SVs). **(a)** When an action potential arrives at the presynaptic terminal, **(b)** voltage-gated Ca^{2+} channels open, which result in Ca^{2+} influx into the presynaptic terminal. **(c)** Neurotransmitters are released into the synaptic cleft by calcium-triggered fusion of SVs with the presynaptic plasma membrane. **(d)** Released neurotransmitters bind to specific neurotransmitter receptors on the postsynaptic cell and activate them, **(e)** which leads to cation or anion (such as Na^+, Ca^{2+} and Cl^-) influx or efflux and excite or inhibit the postsynaptic cell.

1.1. Chemical synaptic transmission

Chemical synapses consist basically of three compartments: (1) a presynaptic nerve terminal, (2) a postsynaptic neuron, typically a cell body or a dendrite of neurons, and (3) a narrow space between the pre- and the postsynaptic membrane called the synaptic cleft. Neurotransmitters are stored in small and round organelles called synaptic vesicles (SVs), which are located within the presynaptic terminals, and are released into the synaptic cleft. Released neurotransmitters diffuse across the synaptic cleft and bind to specific receptors on the postsynaptic membrane, which leads to excitation or inhibition of the postsynaptic cell. The whole process is called synaptic transmission (Figure 1). Synaptic transmission is a fundamental process of brain functions, such as perception, movement, and learning (Kandel et al., 2000).

1.2. Synaptic vesicle cycle

Synaptic transmission relies on neurotransmitter release from presynaptic terminals, which is mediated by Ca^{2+}-triggered fusion of SVs with the presynaptic plasma membrane (exocytosis). Following exocytosis, SV components are retrieved from the plasma membrane into the cytoplasm of presynaptic terminals (endocytosis), which newly regenerate SVs. When new SVs are generated, SV proteins have to be sorted correctly. In addition, endocytosed SVs are acidified by proton influx via proton pumps, such as vacuolar-type H^+-ATPase (V-ATPase; Egashira et al., 2015), and are refilled with neurotransmitters by specific transporters, such as vesicular glutamate transporter (VGLUT; Takamori et al., 2000). New SVs refilled with neurotransmitters are recycled and reused for subsequent rounds of exocytosis (Südhof, 2004).

Thus, as evident, each step in such synaptic vesicle cycle (Figure 2) is precisely controlled, and is essential for sustained synaptic transmission.

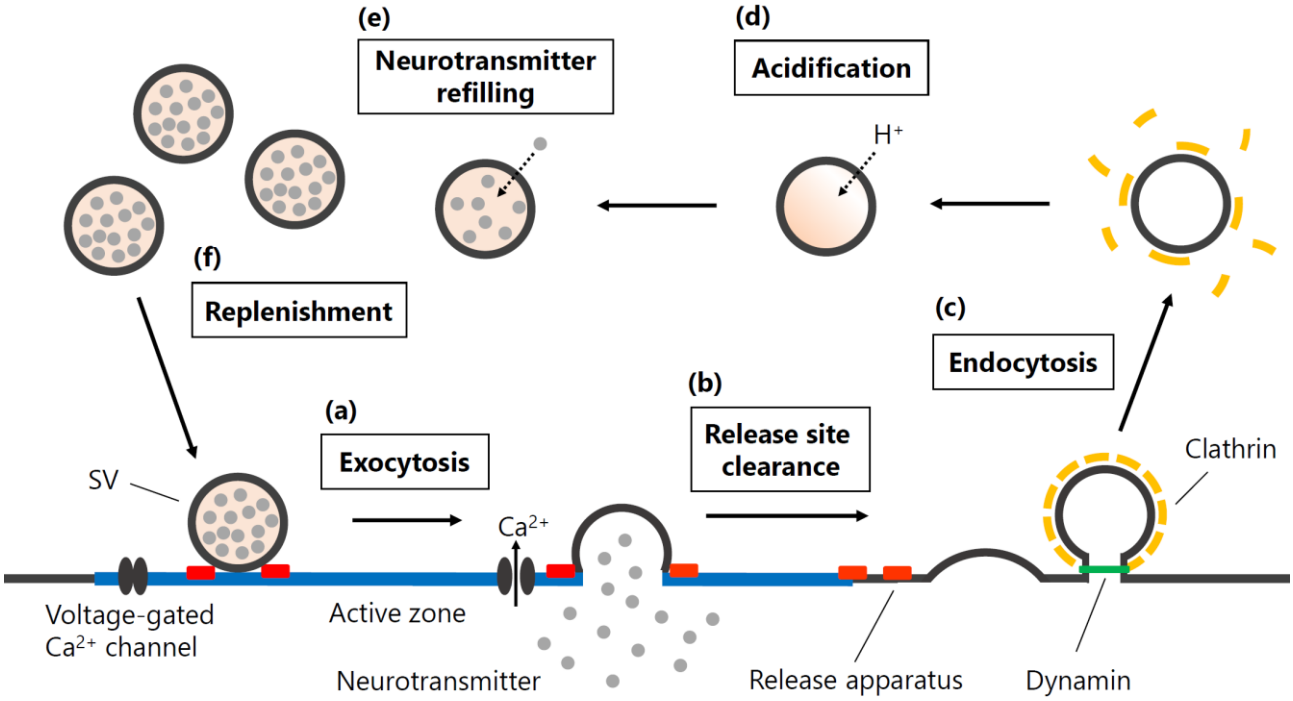

Figure 2. Schematic view of synaptic vesicle cycle at a presynaptic terminal

At the presynaptic terminals, voltage-gated Ca^{2+} channels are clustered at specialized areas called active zones (AZs). SVs are docked at the release sites within the AZs and are ready for exocytosis (priming). **(a)** Ca^{2+} influx through voltage-gated Ca^{2+} channels triggers SV fusion via activating release apparatus such as synaptotagmin and SNARE proteins. Neurotransmitters are released into the synaptic cleft and activate the postsynaptic receptors. **(b)** Exocytosed vesicle membrane and proteins have to be cleared from the AZ to peri-AZ (the area surrounding AZ) to maintain the availability of the release sites. **(c)** Endocytosis of fused SV membrane and proteins occurs at peri-AZs. Dynamin pinches off the clathrin-coated endocytotic intermediates from the presynaptic plasma membrane. **(d)** Following clathrin uncoating, endocytosed SVs are acidified by proton influx **(e)** and are refilled with neurotransmitters. **(f)** New SVs are recruited to the release sites for subsequent rounds of exocytosis.

1.2.1. Synaptic vesicle exocytosis

Action potentials (APs), which are generated at the soma or the axon initial segment, are conducted along axons and arrive at the presynaptic terminal. At the presynaptic terminal, voltage-gated Ca^{2+} channels open in response to an AP. Ca^{2+} influx through the Ca^{2+} channels triggers SV fusion via activation of a putative Ca^{2+} sensor, synaptotagmin1/2 (Brose et al., 1992; Geppert et al., 1994; Xu et al., 2007), which interacts with fusion machinery including SNARE proteins (de Wit et al., 2009;

Zhou et al., 2015). SNARE proteins consist of syntaxin and SNAP-25, which are attached to the plasma membrane, and synaptobrevin/VAMP2, which is a SV protein (Jahn and Scheller, 2006). Association of these three proteins is thought to mediate SV fusion, though the detailed molecular mechanisms remain unclear.

SV fusion is a fast process, which takes place within the time frame of a millisecond (ms; Sabatini and Regehr, 1996). For such a fast process, the fusion machinery has to be intrinsically fast so that molecular machine has to be arranged strategically. In addition, the spatial coupling between Ca^{2+} channels and SVs has to be tight enough to allow fast exocytosis (Eggermann et al., 2012). In the presynaptic terminals, Ca^{2+} channels are clustered at special region called active zones (AZs) (Kulik et al., 2004; Indriati et al., 2013). SVs are docked at the AZs and the docked vesicles are thought to be ready for exocytosis (molecular priming). AZ proteins, such as Rims, Munc13s, Munc18s, CAST, are either relevant for the spatial coupling between Ca^{2+} channels and SVs, and/or molecular priming. Deletion of these proteins gives rise to the phenotype of coupling deficit or priming deficit.

1.2.2. Synaptic vesicle endocytosis

During sustained synaptic transmission, SV exocytosis is repeated over and over. In this process, SV membrane and proteins are continuously added to the release sites. In addition, the supply of SVs for further rounds of exocytosis becomes insufficient, which leads to the depletion of SVs in the presynaptic terminals (Yamashita et al., 2005). To cope with these problems, following vesicle fusion, fused SV components (membrane and proteins) are retrieved from the plasma membrane via endocytosis. Endocytosis is known to have at least four routes/modes: (1) kiss-and-run, (2) clathrin-mediated endocytosis, (3) bulk endocytosis, and (4) ultrafast endocytosis (Figure 3; Wu et al., 2007; Yamashita, 2012; Watanabe et al., 2013; 2014).

(1) In kiss-and-run mode of endocytosis, fused SVs keep their identity and are retrieved rapidly without loosing their form (Fesce et al., 1994). This process takes less than 1 s. Compared

with full collapse of SVs, it is unknown if all the transmitter molecules are released, and SVs may stay in the same place at the AZs and reused repetitively ("kiss and stay" or rapid reuse).

(2) In clathrin-mediated endocytosis, SVs are thought to collapse fully, and clathrin, which is usually located at peri-active zone (peri-AZ), shapes the presynaptic plasma membrane into a vesicular form. It is unknown how the fused SVs (debris) are cleared from the AZ to peri-AZ, but such clearance may be important for another round of exocytosis (Neher, 2010; Haucke et al., 2011). After coating membrane with clathrin, dynamin, a family of GTPases, pinches off the endocytotic vesicles from the presynaptic plasma membrane (Cremona and De Camilli, 1997). Usually, clathrin-

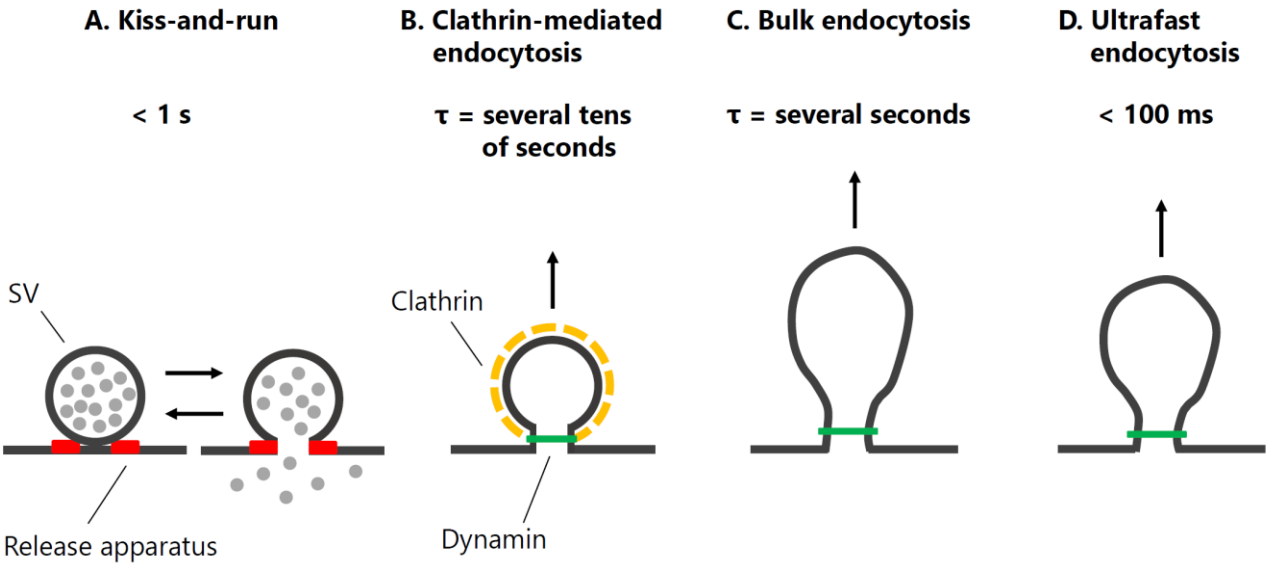

Figure 3. Four modes of synaptic vesicle endocytosis

(A) Kiss-and-run. SVs transiently fuse with presynaptic plasma membrane and are rapidly retrieved without loosing their identity during this process. It has been proposed to be a relatively fast process (τ = less than 1 s).

(B) Clathrin-mediated endocytosis. Following exocytosis, clathrin and dynamin regenerate SVs, and these new SVs take part in another round of exocytosis. This mode of endocytosis takes tens of seconds and is slower process than kiss-and-run.

(C) Bulk endocytosis. Endosome-like, large membrane structures are retrieved in this mode. This process is rapid and takes several seconds. After retrieval, SVs are regenerated from endosome-like structure.

(D) Ultrafast endocytosis. Large vesicles, which are roughly twice as large as the diameter of SVs, are retrieved. This mode of endocytosis takes place within 50 to 100 ms at near physiological temperature (34°C), but fails at room temperature (22°C). Actin and dynamin mediate this form of endocytosis.

mediated endocytosis takes several to tens of seconds, and the identity of SVs is lost during the SV cycle.

(3) In bulk endocytosis, after massive exocytosis endosome-like membrane structure is retrieved to the cytosol (Miller and Heuser, 1984). Bulk endocytosis is considered to be rapid and takes several seconds. After the retrieval of endosome-like structure, SVs are budded and regenerated from these endosomes (Watanabe et al., 2014; Kononenko et al., 2014).

(4) In addition to these three forms of endocytosis, ultrafast endocytosis has been postulated recently, which retrieves large vesicles within 100 ms, with an intermediate size of endosome-like structure (the diameter is approximately 80 nm; Watanabe et al., 2013). Clathrin regenerates SVs from the large endocytotic vesicles 5-6 s after stimulation (Watanabe et al., 2014). This form of endocytosis is mediated by actin and dynamin, and occurs at near physiological temperature (34°C), but fails at room temperature (22°C).

When vesicles lose their identity during exocytosis, SV proteins have to be sorted properly. The exact mechanism of SV protein sorting remains to be unknown but several candidate molecules involved in sorting, such as stonin and intersectin have been postulated to be responsible (Haucke et al., 2011).

In this study, I define “endocytosis" as endocytosis in general, and "retrieval" is defined as endocytosis of specific molecules such as membrane and SV proteins. To avoid confusion, "uptake" is not used in this study, though it is often used to mean the same as retrieval. "Sorting" is defined as sorting of SV proteins in the plasma membrane before endocytosis, so that SV components are retrieved correctly together with the SV membrane.

1.2.3. Synaptic vesicle replenishment

Ca^{2+} influx triggers exocytosis, but the amounts of transmitter release are regulated also by the number of SVs of readily releasable pool (RRP) at the AZ. The number of these SVs is limited, and once all the readily-releasable vesicles are used up (depleted), then synaptic responses exhibit depression. Recovery from depression is determined by the rate of synaptic vesicle replenishment to

the RRP. At the calyx of Held, the number of RRP vesicles is approximately 3000 (Figure 4), and the rate of vesicle replenishment is in the order of hundreds of ms to seconds (Neher and Sakaba, 2008). After release of SVs from RRP at the AZs, new SVs have to be recruited to the AZ for another round of exocytosis. Traditionally, transport of SVs to the release site is rate-limiting, and an important role of AZs is SV recruitment to the AZ. Indeed, some AZ scaffold proteins are thought to play such a role. In addition to vesicle recruitment to the AZs, the number of AZs and release sites is limited in number and the release sites have to be cleared after vesicle fusion. Release sites are cleared by passive diffusion of debris to the peri-AZs or else actively by endocytosis. Recently the site clearance has been postulated to play a major role in synaptic vesicle replenishment, though direct experimental evidence has not been presented (Neher, 2010; Haucke et al., 2011). Below, I describe the site clearance and coupling between exo- and endocytosis in more detail.

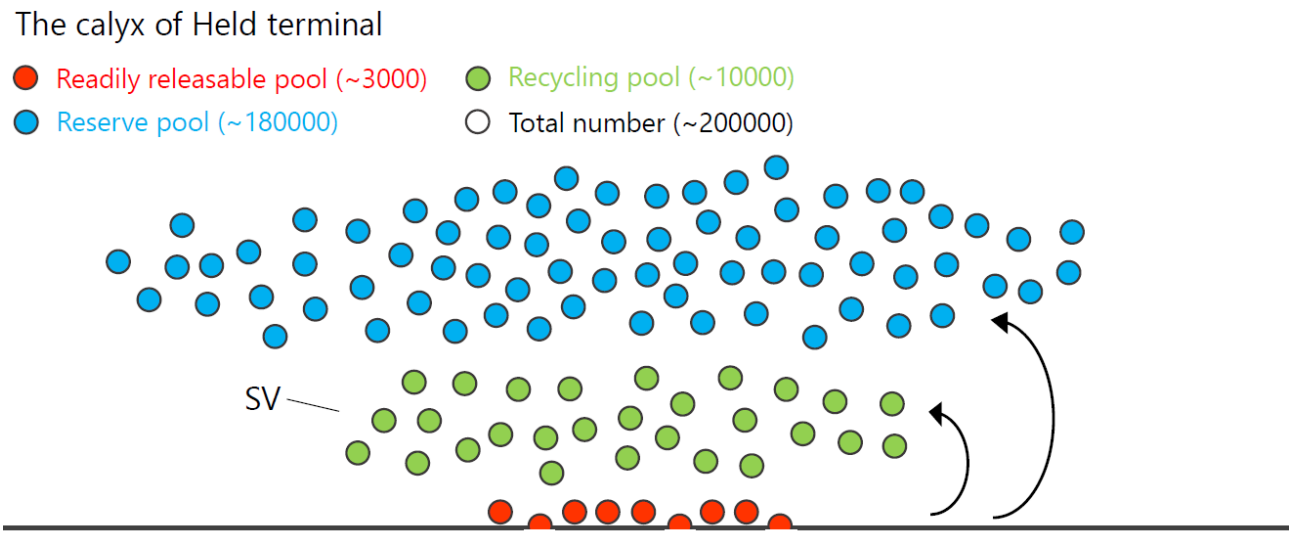

Figure 4. Synaptic vesicle pools

Three SV pools have been postulated: a readily releasable pool (RRP; red), a recycling pool (green), and a reserve pool (blue). RRP consists of SVs which are docked to presynaptic AZs and primed for release. These vesicles are immediately released upon stimulation. The number of SVs in RRP is limited, and once all the readily-releasable vesicles are depleted, then synaptic responses exhibit depression. The recycling pool consists of SVs which are replenished to the AZs after depletion of RRP and released. Recovery from depression is determined by the rate of SV replenishment to the RRP. The vesicles of the reserve pool are reluctant to release, but only recruited upon strong stimulation. Released vesicles are retrieved via endocytosis (black arrows). Endocytosed vesicles may participate in the recycling or the reserve pool.

1.3. Post-fusion process

1.3.1 Clearance of release sites

Endocytosis is essential for SV recycling, but it has been postulated that it is critical for exo-endo coupling at the release sites. As has been described above, for SV replenishment, (1) SVs have to be transported to the release sites, and (2) release sites have to be cleared so that acceptor complex at the release sites (such as syntaxin and SNAP-25) can accept new SVs (Neher and Sakaba, 2008; Haucke et al., 2011). It is considered that released materials (SV proteins or dead SNARE complex) have to be cleared from the release sites at AZs to peri-AZs, which surrounds the AZs and is the site for endocytosis (Haucke et al., 2011). It has not been directly shown, however, if such clearance happens. So far, more indirect observations have been obtained. For example, blocking of endocytosis by dynamin and AP-2 inhibitors delays SV replenishment at the calyx of Held synapse (Hosoi et al., 2009) and hippocampal synapse in culture (Hua et al., 2013), consistent with the idea that the site clearance through endocytosis is important for SV replenishment. At the calyx of Held, it has been shown that pharmacological block of calmodulin slows SV replenishment (Sakaba and Neher, 2001) and that mutation of calmodulin-binding site of Munc13-1 slows SV replenishment as well (Lipstein et al., 2013). Although Munc13-1 is considered to be a priming protein, which is essential for SV priming before fusion, it has not been shown that Munc13-1 regulates the retrieval of SV membrane and/or of SV proteins. In this study, by monitoring retrieval of synaptotagmin2, a SV protein, I examined if this is the case.

1.3.2 Sorting of SV proteins

After clearance of SV proteins from the release sites to peri-AZ (endocytotic zone), SV proteins have to be sorted so that endocytosis properly retrieves membrane and SV proteins in a coordinated manner (Haucke et al., 2011). In addition, the presence of a readily retrievable pool of SV proteins at the peri-AZ has been postulated, where endocytosis takes place (Hua et al., 2011). Several endocytotic proteins, such as AP-2 (Traub, 2009), AP180 (Koo et al., 2011), endophilin (Milosevic et al., 2011), or stonin 2 (Kononenko et al., 2013), were proposed as potential adaptors for endocytocic vesicle

protein sorting, but the detailed mechanisms are still debated (Opazo and Rizzoli, 2010). A clear separation between sorting and clearance is difficult, because sorting may also clear the released materials from AZs. If so, they might occur at the same time. Synaptic vesicle sorting is required because synaptic vesicles are recycled within tens of seconds (Rizzoli and Betz, 2005), and SVs cannot be fusion competent in such a time scale if random incorporation of SV proteins happens during endocytosis and SV proteins have to be correctly sorted after endocytosis .

1.4. Coupling between exo- and endocytosis

After synaptic vesicle sorting (Haucke et al., 2011), endocytosis takes up the SV membrane and proteins. As for membrane retrieval, capacitance measurements revealed a fast and a slow endocytosis component. Fast endocytosis with a time constant of less than a few seconds, is seen when a strong stimulus is applied (Xue et al., 2012), and often involves excess membrane retrieval. In contrast, slow endocytosis, which is a major form of endocytosis, has a time constant of seconds to tens of seconds, and at a variety of synapses, the amount of membrane endocytosed in this manner is similar to the amount of membrane that had previously been exocytosed (von Gersdorff and Matthews, 1994; Moser and Beutner, 2000; Sun and Wu, 2001). Subsequent studies showed that fast and slow endocytosis reflects clathrin-independent and clathrin-dependent modes of endocytosis, respectively (Wu et al., 2009; Yamashita et al., 2010), and that the contribution of fast endocytosis increased progressively when stimulus intensity was increased (Renden and von Gersdorff, 2007; Wu et al., 2009; Yamashita et al., 2010; Midorikawa et al., 2014). Control of the kinetics and the amount of the membrane retrieval has high physiological relevance, since perturbation of the membrane retrieval induces use-dependent depletion of the releasable vesicles and rundown of exocytosis (Yamashita et al., 2005) and release site clearance may be important for subsequent exocytosis as described above (see also Haucke et al., 2011).

The maintenance of transmitter release is not only dependent on membrane retrieval following membrane fusion, but also on the recovery of vesicular proteins into the recycling vesicles (Kononenko and Haucke, 2015). Vesicle protein recycling has been studied mainly by using a pH-

sensitive green fluorescent protein (GFP) variant, pHluorin, as a vesicle protein marker (Miesenböck et al., 1998). Except for kiss-and-run events, retrieval of vesicular proteins seems to be slow, with a time constant of seconds to tens of seconds, similar to the time constant of membrane retrieval during slow endocytosis as assessed by capacitance measurements. However, in contrast to membrane retrieval that gets faster as stimulation persists (because fast endocytosis is triggered by massive stimulation), the retrieval of synaptic proteins slows down as stimulation persists (Armbruster et al., 2013; Fernández-Alfonso and Ryan, 2004). Further, exocytosed vesicular proteins, such as VAMP2 (Sankaranarayanan and Ryan, 2001; Gandhi and Stevens, 2003), synaptophysin (Granseth et al., 2006), synaptotagmin (Fernández-Alfonso et al., 2006), and VGLUT (Balaji and Ryan, 2007), appear to be retrieved into endocytotic organelles to similar extents. Proper endocytotic retrieval is of high physiological relevance, given that clearance of vesicle proteins from transmitter release sites may be required for the maintenance of synaptic transmission and that insufficient retrieval leads to the slowed recruitment of SVs to release sites (Hosoi et al., 2009; Wu et al., 2009; Hua et al., 2013).

To gain detailed insight into the mechanisms of membrane and vesicular protein retrieval, simultaneous measurements of membrane retrieval and vesicle protein retrieval are required that allow for the separate assessment of membrane retrieval kinetics and vesicle protein retrieval kinetics in the same presynaptic terminal. Such simultaneous measurements would allow us to address the known kinetic differences between capacitance measurements and pHluorin-based measurements.

1.5. Three techniques to study synaptic vesicle endocytosis

SV cycling has been studied for decades using electron microscopy, membrane capacitance measurements, and live imaging of fluorescent markers. Below I have described each technique.

1.5.1. Electron microscopy

Though images are static, putative endocytosis has been captured by electron microscopy. Heuser and Reese (1973) have discovered omega-shaped membrane structures at peri-AZs and clathrin-coated vesicles at frog neuromuscular junction, which led them to postulate that these structures represent

endocytosis. Also, using electron microscopy, Ceccarelli and colleagues (1973) postulated that vesicles are retrieved without losing their shape and identity, which is considered to be the first evidence for kiss-and-run. More recently, by using flash-and-freeze technique, Watanabe et al. (2013) have provided evidence of ultrafast endocytosis, which retrieves membrane within hundreds of ms with an intermediate size of an endosome-like structure. Although electron microscopy provides only a "snap-shot" picture, it has very high spatial resolution, and gives valuable information regarding various forms of endocytosis. In this thesis, electron microscopy technique was not used because I aimed to investigate the kinetics of endocytosis of membrane and vesicular proteins by simultaneous real-time recordings.

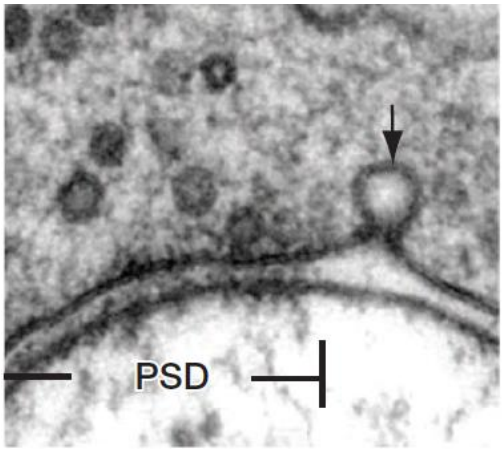

Figure 5. Endocytotic pit of ultrafast endocytosis by electron microscopy
The example micrograph showing invagination in the peri-AZ at 100 ms after stimulation. Arrow indicates the omega-shaped structure (endocytotic pit) of ultrafast endocytosis. Image from Watanabe et al. (2013).

1.5.2. Membrane capacitance measurements

Neher and Marty (1982) developed the capacitance measurements: Exo- and endocytosis involve an increase or a decrease in the membrane surface area, which can be measured as changes in the membrane capacitance. It was first applied to secretory cells such as neuroendocrine cells, and subsequently, it was applied to neuronal synapses such as retinal bipolar cells (von Gersdorff and Matthews, 1994), hair cells (Lenzi et al., 1994) and the calyx of Held synapse (Sun and Wu, 2001). Capacitance measurements provide real-time monitoring of endocytosis with high temporal resolution (time scale of ms), but cannot provide any spatial information where and how endocytosis takes place on a microscopic scale. Also, due to large conductance changes, one cannot measure exo- and endocytosis when ionic channels are activated, such as during depolarization. In addition,

capacitance measurements measure the net balance of exo- and endocytosis, so they have to be temporally decoupled.

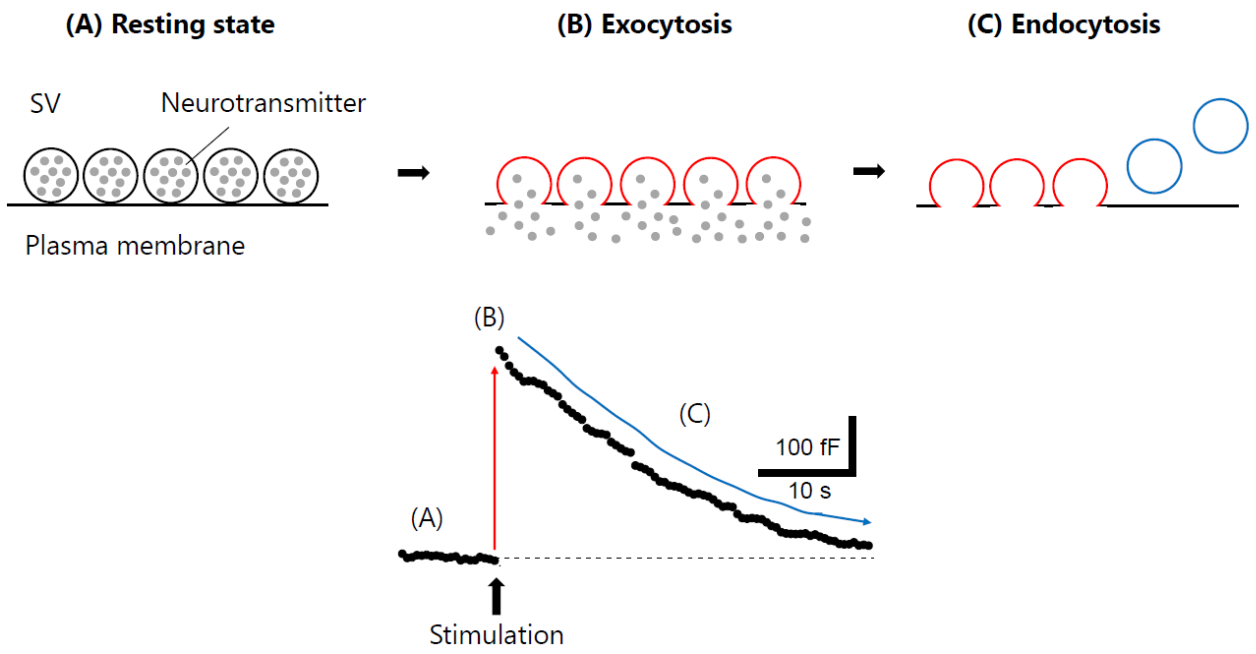

Figure 6. Monitoring of membrane endocytosis by membrane capacitance measurements
(Top) Scheme of SV exo- and endocytosis. Exo- and endocytosis of SVs involve an increase or a decrease in the membrane surface area, and membrane capacitance is proportional to the membrane surface area. Therefore, exocytosis of SVs elicited by stimulation leads to capacitance increment and endocytosis of SVs leads to capacitance decrement. Exo- and endocytosis of SVs can be measured as changes in the membrane capacitance of presynaptic terminal.
(Bottom) An example trace of capacitance measurements at the calyx of Held terminal. (A) Resting membrane capacitance is stable before stimulation. (B) When the calyx terminal is stimulated by a depolarizing pulse (0 mV for 50 ms following a prepulse to +70 mV for 2 ms), SVs fuse with the presynaptic plasma membrane leading to capacitance increment. (C) Following exocytosis, SVs are retrieved by endocytosis, membrane capacitance gradually decrease.

1.5.3. Live imaging using fluorescent markers

In the early 1990s, Betz and colleagues have used styryl dyes such as FM1-43 to stain SVs and monitor their dynamics (Betz and Bewick, 1992). It was inserted to membrane, taken up to the cell by endocytosis and SVs were stained. By using different stimulation patterns, different forms of endocytosis were observed, such as clathrin-mediated endocytosis, kiss-and-run, and bulk

endocytosis. In the late 1990s, pH-sensitive GFP or its variant has been developed (Miesenböck et al., 1998), which was conjugated to SV proteins (synaptopHluorin, for example). In the vesicle lumen pH is usually below 6 (acidic), and when SVs are exocytosed, then pH becomes neutral (~7). pH-sensitive GFPs change their fluorescent, depending on the state of vesicles (if they are in the cytosol, or if they are exocytosed). In the same way, pH-sensitive cyanine dye, cypHer5E, is also used (Hua et al., 2010, 2011, 2013). pH-sensitive dye (such as cypHer) is conjugated to the antibody, which recognizes the luminal domain of SV proteins. Then, depending on the state of SVs, changes in fluorescence are observed. Imaging method provides spatial and temporal information on vesicle dynamics, but temporal resolution is somewhat limited compared with capacitance measurements, and spatial resolution is not as good as electron microscopy. In addition, GFP- or antibody-based optical measurements monitor the dynamics of SV proteins, whereas capacitance measurements monitor the dynamics of SV membrane. Nevertheless, all three methods are complementary to each other. An important point, here, is that there are few studies which combine more than two techniques. In this study I tried to combine capacitance measurements with optical measurements.

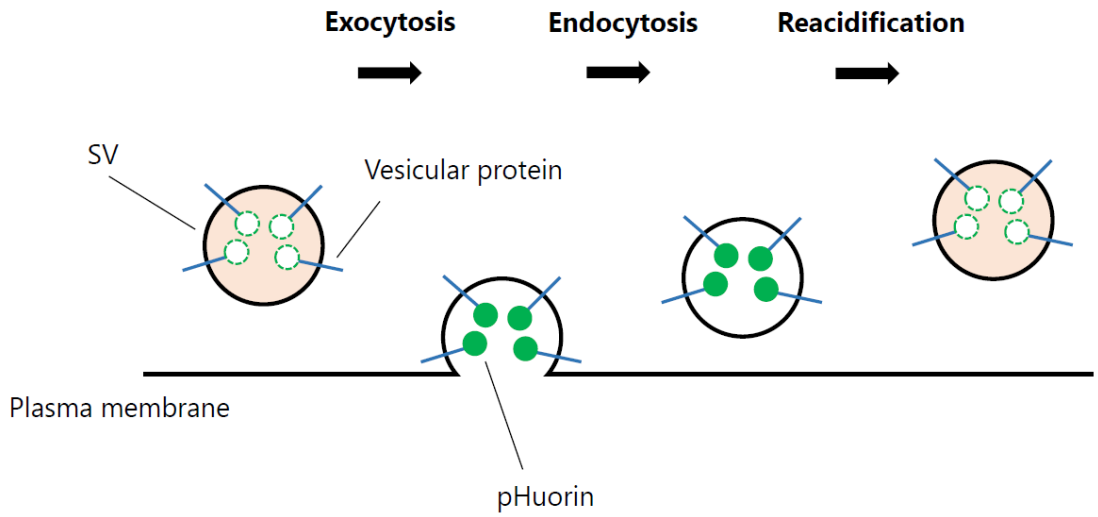

Figure 7. Monitoring of vesicular protein endocytosis using pHluorin
pHluorin is a pH-sensitive GFP, and this molecule can be attached to the luminal domain of vesicular proteins such as synaptobrevin and synaptophysin. The luminal pH of SVs is normally acidic (approximately 5.5), at which point the fluorescent signal of pHluorin is quenched. When SVs are exocytosed, the lumen of SVs are exposed to the extracellular pH (~7.4), which causes an increase in its fluorescence. The fluorescent signal of pHluorin is quenched again after endocytosis by reacidification of SVs.

1.6. The calyx of Held in the auditory brainstem

The calyx of Held synapse is a mammalian model system of synaptic transmission at central synapses (Forsythe, 1994; Borst and Sakmann, 1996; Wu and Borst, 1999). The large terminal size (10-20 μm) enables simultaneous voltage-clamp recordings from pre- and postsynaptic compartments, so that the kinetics of exocytosis can be dissected (Wu and Borst, 1999; Sakaba and Neher, 2001). In addition, the extent and the time course of membrane fusion and retrieval can be monitored by membrane capacitance measurements (Sun and Wu, 2001). Correspondingly, the calyx of Held is one of the best characterized synapses as regards the relationship between the kinetics of exo- and endocytosis. However, the dynamics of synaptic vesicle protein retrieval has remained unclear at the calyx synapse because optical measurements have not been applied.

1.7. The aim of this study

This study has two purposes: (1) By simultaneous monitoring of membrane dynamics and protein dynamics at the calyx of Held synapse, I compared the retrieval kinetics of membranes and vesicular proteins. Previous studies did not perform simultaneous measurements of membrane and SV proteins retrieval, and it is important to examine whether membrane and SV proteins are retrieved in a coordinated manner. Specifically, I explored why the kinetics are different between capacitance measurements and optical measurements: Membrane retrieval gets faster with stronger stimulation whereas SV proteins retrieval gets slower with stronger stimulation. To monitor the dynamics of SV proteins retrieval at the calyx terminal, I used the cypHer5E fluorophore (referred hereafter as cypHer; Adie et al., 2003; Hua et al., 2011), as an exo-endocytosis reporter. The cypHer moiety, which has a pH dependence opposite to pHluorin (i.e. fluorescent in acidic pH, and quenched in neutral pH), was coupled to antibodies against the luminal domain of synaptotagmin 2 (anti-Syt2-cypHer), an endogenous SV protein at the calyx of Held terminal (Pang et al., 2006), so that my strategy directly labels an endogenous Syt2 with cypHer. Syt2 was chosen because it is an important SV protein and anti-Syt2-cypHer is already available (Hua et al., 2011). I discovered two modes of membrane and protein retrieval depending on stimulus intensities, and both are retrieved in a coordinated manner.

(2) I addressed whether SV membrane and proteins are controlled all together or could be controlled independently. I identified Ca^{2+}-calmodulin-Munc13-1 signaling pathway regulates the retrieval of SV proteins, independent of membrane retrieval. I discussed the results in terms of functional significance (such as clearance of release sites).

2. Materials and Methods

2.1. Ethical approval

Animal care and animal procedures were conducted in accordance with the guidelines of the Physiological Society of Japan, and were approved by the Doshisha University Committee for Regulation on the Conduct of Animal Experiments and Related Activities. All efforts were taken to minimize animal numbers. The generation, maintenance, and use of the Munc13-1^{W464R} mice were approved by the responsible local government organization (Niedersächsisches Landesamt für Verbraucherschutz und Lebensmittelsicherheit, permissions 33.9.42502-04-13/1359 and 33.19-42502-04-15/1817).

2.2. Brainstem slice preparation

Transverse brainstem slices (200 μm thickness) were prepared from 9- to 11-day-old Wistar rats, C57BL6 mice, Munc13-1^{W464R} KI mice, and wild type littermates (Munc13-1^{WT}) of either sex using a Leica VT1200S slicer (Leica Microsystems, Wetzlar, Germany). Animals were anesthetized with isoflurane (Wako, Japan) and rapidly decapitated. After removing the skin and opening the skull, the brain was removed from the skull and carefully placed in ice-cold sucrose-based solution containing (in mM) 130 Sucrose, 60 NaCl, 2.5 KCl, 25 glucose, 25 $NaHCO_3$, 1.25 NaH_2PO_4, 0.5 ascorbic acid, 3 myoinositol, 2 Na-pyruvate, 0.1 $CaCl_2$, and 3 $MgCl_2$ (pH 7.4, gassed with 95% O_2 and 5% CO_2). The brainstem and cerebellum were removed and then glued to the stage of the slicer. Four to five transverse brainstem slices were cut sequentially from the level of the seventh nerve at 200 μm thickness. The brainstem and cerebellum were kept in ice-cold sucrose-based solution during slicing. In order to allow slices to recover from the cutting procedure, slices were incubated at 37°C for 1 hr in a maintenance chamber filled with extracellular solution containing (in mM) 125 NaCl, 2.5 KCl, 25 glucose, 25 $NaHCO_3$, 1.25 NaH_2PO_4, 0.4 ascorbic acid, 3 myoinositol, 2 Na-pyruvate, 2 $CaCl_2$, and 1 $MgCl_2$ (pH 7.4, gassed with 95% O_2 and 5% CO_2).

2.3. Anti-Syt2-cypHer labeling

CypHer5E dye conjugated to antibodies directed against the luminal domain of Syt2, anti-Syt2-cypHer (Synaptic Systems, Göttingen, Germany), was used to monitor exo-endocytosis from the calyx presynaptic terminal. To label the calyx of Held terminals, slices were incubated with anti-Syt2-cypHer at 37°C for 30 min in a high K^+ solution containing (in mM) 95 NaCl, 32.5 KCl, 25 glucose, 25 $NaHCO_3$, 1.25 NaH_2PO_4, 0.4 ascorbic acid, 3 myoinositol, 2 Na-pyruvate, 2 $CaCl_2$, and 1 $MgCl_2$ (pH 7.4). The high K^+ solution results in depolarization of the membrane potential of presynaptic terminals due to the increase in the equilibrium potential of potassium. This depolarization opens voltage-gated Ca^{2+} channels and induces exo- and endocytosis of SVs. Therefore, anti-Syt2-cypHer recognized the luminal domain of Syt2 and were internalized to SVs. CypHer has a pH dependence opposite to pHluorin (i.e. fluorescent in acidic pH, and quenched in neutral pH), so that the fluorescence of cypHer is quenched upon exocytosis because of the exposure to the extracellular pH and de-quenched again upon endocytosis and subsequent re-acidification. Subsequently, slices were held at 37°C for up to 3 hrs in the extracellular solution until mounting onto an upright microscope (Axioskop; Zeiss, Oberkochen, Germany).

2.4. Whole-cell voltage clamp recordings

Slices were individually transferred to a recording chamber perfused with the extracellular solution and visualized on the upright microscope. The extracellular solution was not perfused during recording to avoid pipette drifting. Patch pipettes were pulled from borosilicate glass capillary (outer diameter: 1.5 mm, inner diameter: 0.86 mm, length: 10 cm; Harvard Apparatus, Holliston, Massachusetts) with a vertical pipette puller (Narishige, Tokyo, Japan). The calyx of Held presynaptic terminals were whole-cell voltage clamped at -80 mV using an EPC9/2 amplifier (HEKA, Lambrecht, Germany) controlled by PatchMaster software (HEKA). The presynaptic patch pipettes (7-10 MΩ) were filled with intracellular solution containing (in mM) 140 Cs-gluconate, 20 TEA-Cl, 10 HEPES, 5 Na_2-phosphocreatine, 4 MgATP, 0.3 NaGTP, and 0.5 EGTA (pH 7.3). When using calmodulin/dynamin inhibitory peptide, both reagents were added to the intracellular solution. For

recordings of wild type mice, 5 out of 8 data were taken from C57BL6 mice with CsCl-based intracellular solution, in which Cs-gluconate was replaced by CsCl. 3 out of 8 data were taken from Munc13-1^{WT} mice with Cs-gluconate-based intracellular solution. Since we found no difference by using CsCl-based intracellular solution, I pooled the corresponding data.

The presynaptic series resistance (10-25 MΩ) was compensated by 10-50% as appropriate. During recordings, 1 μM TTX and 10 mM TEA-Cl were included in the extracellular solution to block Na^+ and K^+ channels respectively, and presynaptic Ca^{2+} currents were isolated. Only cells with stable membrane resistance (Rm), leak current below 50 pA at holding potential (-80 mV) and stable series resistance below 25 MΩ were considered in the study.

2.5. Capacitance measurements

Membrane capacitance measurements from the calyx of Held presynaptic terminals were performed using an EPC9/2 amplifier in the sine+DC configuration (Lindau & Neher, 1988). A sine wave (30 mV in amplitude, 1000 Hz in frequency) was superimposed on a holding potential of -80 mV. A train of depolarizing pulses (+70 mV for 2 ms followed by repolarization to 0 mV for 50 ms, repeated ten times with an inter-stimulus interval of 200 ms) and a step depolarizing pulse (+70 mV for 2 ms followed by repolarization to 0 mV for 2 s) were used to evoke Ca^{2+} currents and exocytosis of SVs in between sine wave. During capacitance measurements, time-lapse fluorescence imaging was recorded simultaneously (see as below). Experiments were performed at room temperature (~25°C). TTX and bafilomycin were obtained from Wako (Osaka, Japan). MgATP, NaGTP, and TEA-Cl were obtained from Sigma-Aldrich (St. Louis, Missouri). The calmodulin and dynamin inhibitory peptides were from Calbiochem (Darmstadt, Germany). Other reagents were from Nacalai tesque (Kyoto, Japan).

2.6. Fluorescence imaging

Experiments were performed at room temperature (~25°C) on an upright microscope (Axioskop, Zeiss) equipped with a 60x, 0.9 NA water-immersion objective (Olympus, Tokyo, Japan). Images

(1344 x 1024 pixels) were acquired with a CCD camera (ORCA-R2 Digital CCD camera C10600; Hamamatsu Photonics, Shizuoka, Japan) controlled by HoKaWo software (Hamamatsu Photonics). Anti-Syt2-cypHer was excited at 645 nm with a monochromator (Polychrome V; Till Photonics, Hillsboro, Oregon) triggered by PatchMaster software (HEKA) and imaged using a 692/40 nm single-band bandpass filter (Semrock, Rochester, New York). Time-lapse images were acquired at 0.5 Hz with 300-500 ms exposure time. Sample rates were determined by signal-to-noise ratio and minimalizing photobleaching. Time-lapse images were corrected for photobleaching by subtracting the bleaching time course of the neighboring calyx terminal (Figure 8). The fluorescence intensity of the region of interest (ROI) was background-subtracted, and normalized either to initial intensity or to ΔF induced by stimulation.

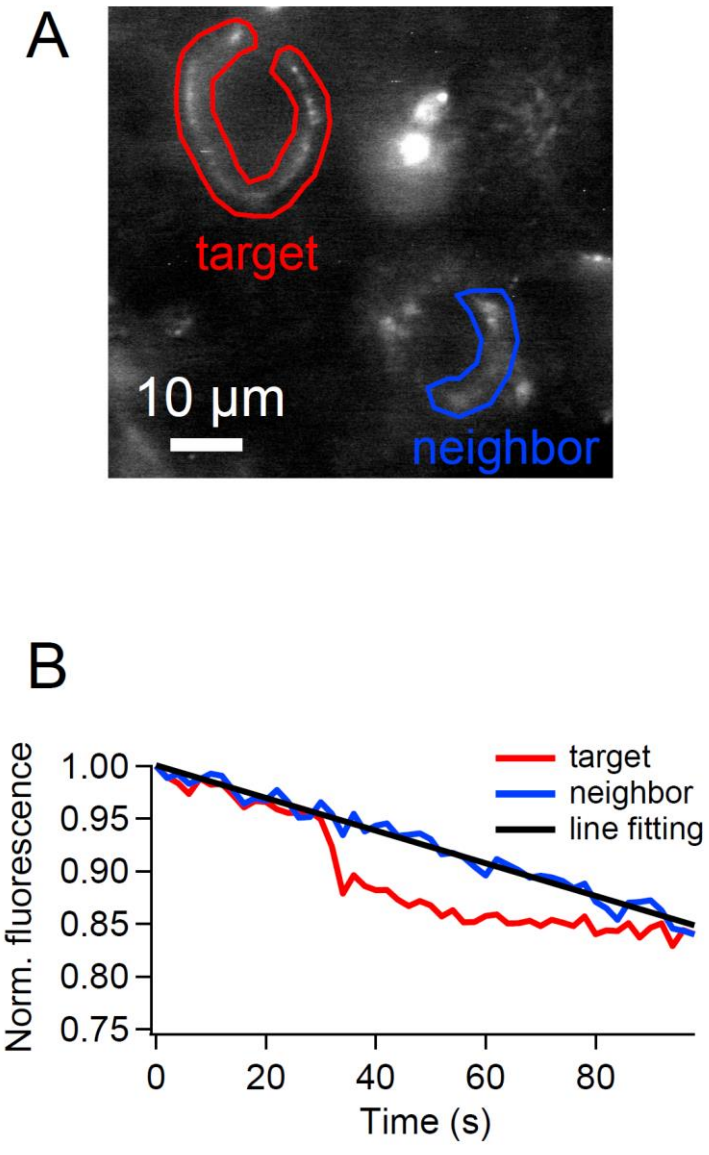

Figure 8. Bleach correction for the cypHer fluorescence

A. Bleach was corrected based on the fluorescence of a neighboring unstimulated calyx.

B. Fluorescence intensity of the ROI was normalized after background subtraction, and the line (or exponential) was fitted to the neighboring calyx fluorescence. The fitted line (or exponential) was subtracted from the target calyx fluorescence.

To monitor fluorescence changes during exo-endocytosis, the calyx of Held terminals were stimulated with a train of depolarizing pulses (+70 mV for 2 ms followed by repolarization to 0 mV for 50 ms, repeated ten times with an inter-stimulus interval of 200 ms) and a step depolarizing pulse (+70 mV for 2 ms followed by repolarization to 0 mV for 2 s). For experiments involving the application of acidic solutions, MES-buffered (25 mM) extracellular solution at pH 5.5 was puff-applied to target terminals using a Pneumatic PicoPump (World Precision Instruments, Sarasota, Florida) before and after stimulation. The MES-buffered solution was made by replacing 25 mM $NaHCO_3$ of the standard external solution to 25 mM MES. The puff pipette (4-6 MΩ) was positioned ~100 μm away from the target terminal.

2.7. Generation of Munc13-1^{W464R} KI mice

Munc13-1^{W464R} KI mutant mice were generated as described previously (Lipstein et al., 2013). In these mice, a point mutation in exon 11 of the *Unc13a* gene replaces the tryptophan in position 464 of Munc13-1 by an arginine and produces a Munc13-1 mutant that does not bind CaM (Junge et al., 2004; Lipstein et al., 2013). Wild type littermates (Munc13-1^{WT}) were used as controls, and the genotypes of the mice were determined by PCR before and after the experiments.

2.8. Image and data analysis

Images and data were analyzed using IGOR Pro 6 (WaveMetrics, Lake Oswego, Oregon) and Excel 2013 software (Microsoft, Redmond, Washington). Patched terminals were defined as ROI and surrounding region was used for background subtraction. Then, average signal intensity was calculated to measure fluorescent changes. In Figure 11 and 21, cypHer signals were fitted by assuming some delay in re-acidification and some re-acidification time constant after membrane retrieval (dotted line). This means that for each endocytotic vesicle, there is a delay before re-acidification, and re-acidification has an exponential time constant. Because endocytosis time course takes the time constant of tens of seconds, recovery of the cypHer signals is convolution of all three parameters (membrane retrieval, delay in re-acidification and acidification). This analysis assumes

that Syt2 is retrieved together with membrane simultaneously. I should point out that the exact estimation of the rate of Syt2 retrieval and reacidification is difficult in this study.

All values are given as mean ± SEM. Statistical significance was determined by Student's t test. p values smaller than 0.05 were considered to indicate statistically significant differences.

The pH-dependence of the cypHer fluorescence was described by a Henderson-Hasselbalch equation with a Hill coefficient of 1, and a pKa of 7.05 (Hua et al., 2011).

3. Results

3.1. Simultaneous recordings of membrane capacitance and anti-Syt2-cypHer retrieval

To visualize the turnover of the vesicular protein Syt2, I labeled calyx terminals with anti-Syt2-cypHer in a slice preparation (Figure 9A).

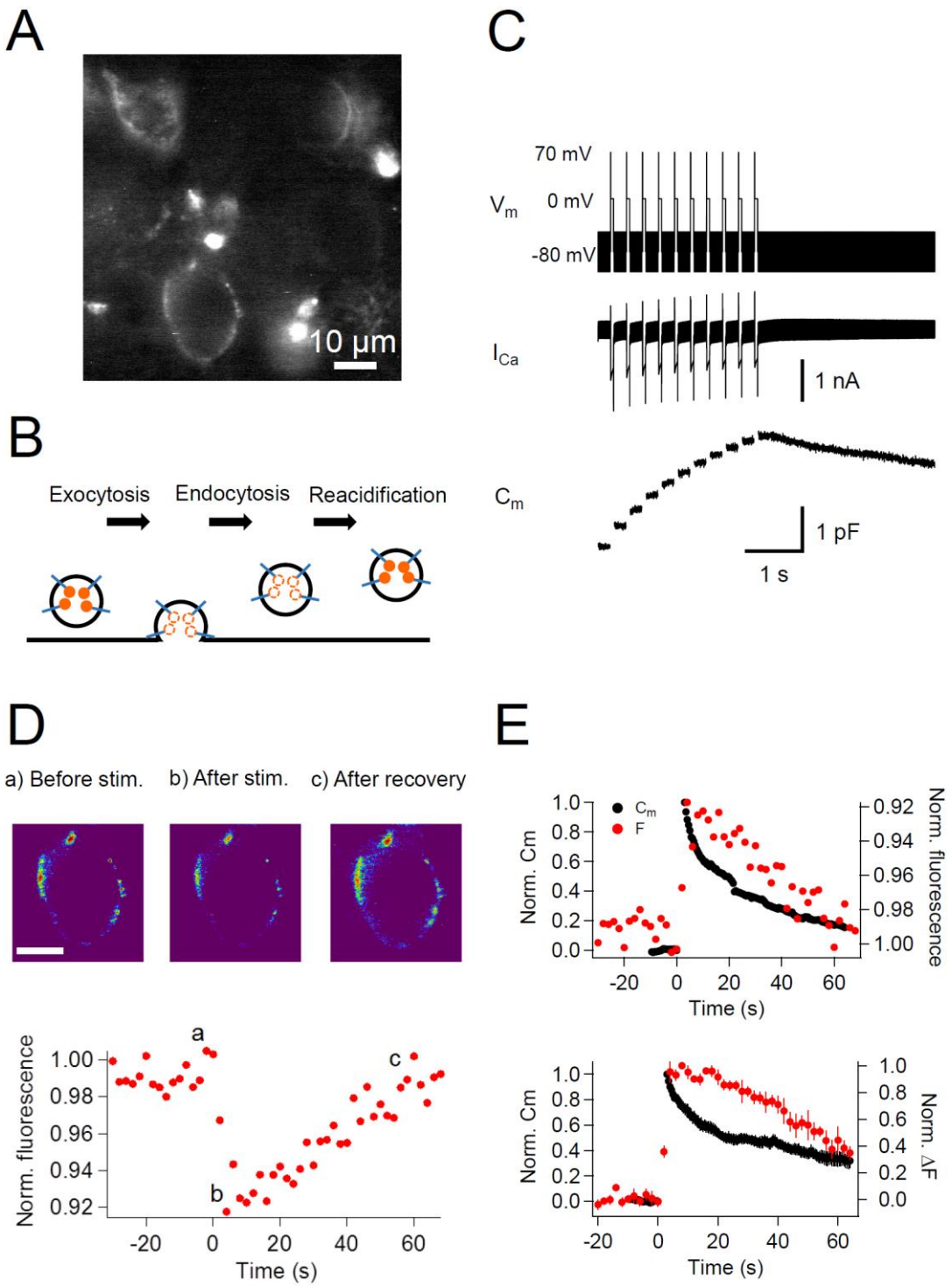

Figure 9. Simultaneous recording of membrane capacitance and anti-Syt2-cypHer fluorescence

(A) Example fluorescence image of calyx of Held presynaptic terminals labeled with anti-Syt2-cypHer. Intravesicular anti-Syt2-cypHer emits fluorescence upon excitation at 645 nm.

(B) Schematic view of fluorescence changes of anti-Syt2-cypHer during exo-endocytosis. The orange dots show cypHer coupled to antibodies against the luminal domain of Syt2. The cypHer fluorescence is maximal at intravesicular pH 5.5 and almost quenched at the extracellular pH 7.4. Upon exocytosis, the fluorescence is quenched because of the exposure to the extracellular pH. During endocytosis and re-acidification, the fluorescence is de-quenched again.

(C) A train of depolarizing pulses (0 mV for 50 ms following a prepulse to +70 mV for 2 ms, 10 stimuli, interstimulus interval 200 ms, V_m) was applied to elicit a Ca^{2+} current (I_{Ca}), and membrane capacitance (C_m) was measured during the sweep. The prepulse (+70 mV) was applied to activate Ca^{2+} channels maximally without causing Ca^{2+} influx. A sine wave (30 mV in amplitude, 1000 Hz in frequency) was superimposed on a holding potential of -80 mV to measure membrane capacitance (C_m).

(D) The top panel shows example fluorescence images showing the cypHer fluorescence image (a) before stimulation, (b) after stimulation, and (c) after recovery, shown in a pseudo-colored scale. Each image was taken at the time point shown in the bottom trace. Scale bar, 10 μm. The bottom panel shows an example of a normalized fluorescence trace of anti-Syt2-cypHer in response to a train of depolarizing pulses. The fluorescence intensity was normalized to the first point in the plot.

(E) The top panel shows example traces of normalized C_m (black circles, left axis) and cypHer fluorescence (red circles, right axis) at a calyx terminal stimulated by a train of depolarizing pulses. The C_m trace was normalized to the amplitude of the capacitance jump, and the fluorescence trace was normalized to the initial intensity. The fluorescence trace was inverted to compare the time courses of C_m and fluorescence traces. The bottom panel shows average traces of normalized C_m (black circles, n = 7) and cypHer fluorescence change (red circles, n = 10) at the calyx terminal evoked by a train of depolarizing pulses (7 data were obtained from simultaneous measurements of capacitance and cypHer). C_m traces were normalized to the peak capacitance change (left axis), and fluorescence traces were normalized to the peak fluorescence change (right axis).

The 200 μm transverse brainstem slices were incubated for 30 min in a high potassium solution (32.5 mM) containing anti-Syt2-cypHer (0.01 mg/ml) to depolarize the terminals and induce exocytosis followed by endocytosis, in which the anti-Syt2-cypHer is internalized (Figure 9B). The fluorescence of the cypHer dye is almost quenched at the neutral extracellular pH of 7.4 after SV exocytosis and is almost maximal at the intravesicular pH of 5.5 (Hua et al., 2011). Therefore, the cup-shaped

structures observed in Figure 9A can be assumed to be calyx terminals filled with anti-Syt2-cypHer-containing internalized vesicles. The staining was calyx specific in this region, and anti-Syt2-cypHer showed a stimulus dependent fluorescence change when field stimulations were applied (Figure 10; Hua et al., 2011). Anti-Syt2-cypHer exposed to the membrane surface is barely fluorescent, so that background fluorescence is kept low even in a slice preparation. To measure the kinetics of Syt2 and

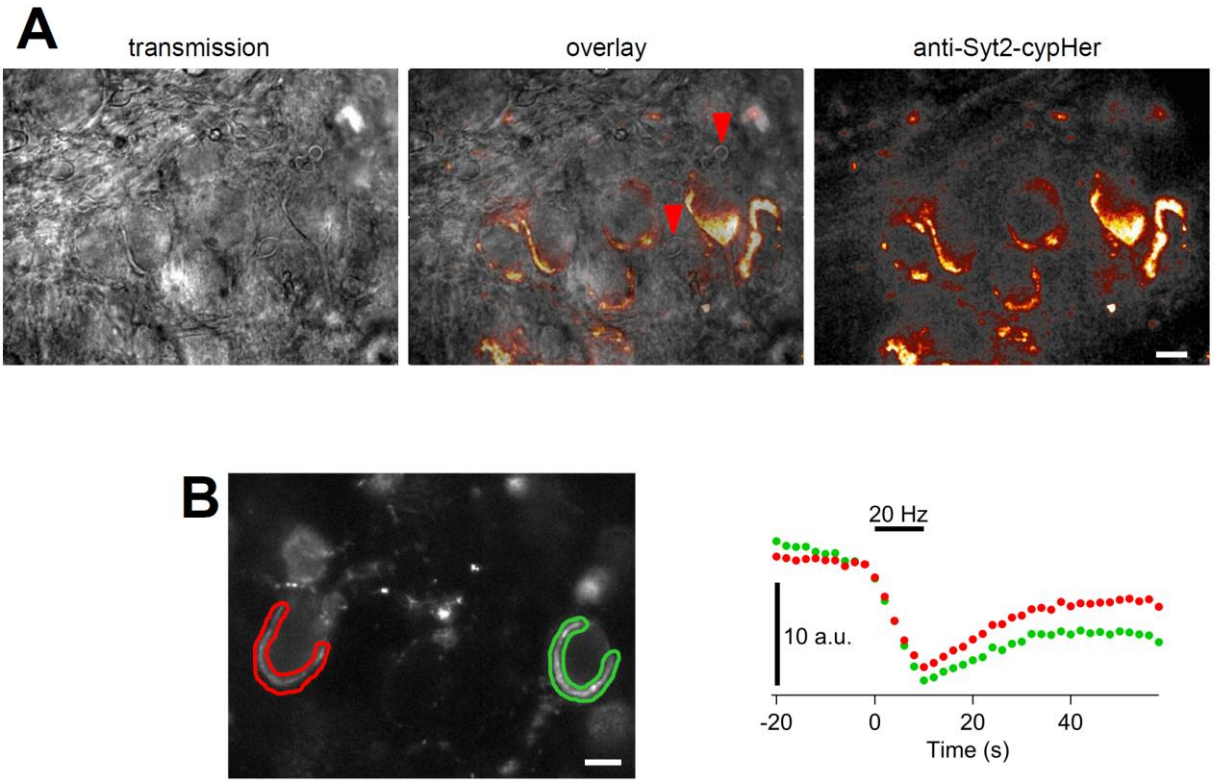

Figure 10. Calyx specific anti-Syt2-cypHer staining and fluorescence change evoked by field stimulation

(A) Transmission image (left), and anti-Syt2-cypHer fluorescent image (right) in the MNTB region of the rat brainstem slice. The center shows an overlay.

(B) A series of field stimulations (20 Hz for 10 s) was applied to the anti-Syt2-cypHer labeled slice (left). The fluorescence intensity at the ROIs is shown on the right. The apparent partial recovery is likely to be due to photobleaching (Hua et al., 2011). Scale bars, 10 μm.

plasma membrane retrieval simultaneously, labeled calyx terminals were whole-cell voltage clamped, and the membrane capacitance and the cypHer signal were measured. When the terminal was stimulated with a train (10 times, 200 ms intervals) of depolarization pulses (0 mV for 50 ms following a prepulse to +70 mV for 2 ms), large capacitance jumps caused by exocytosis were observed (1.52 ± 0.21 pF after 10 pulses, n = 7, Figure 9C). A 50 ms pulse is sufficient to deplete the

readily releasable pool of SVs (Hosoi et al., 2009; Wu et al., 2009; Yamashita et al., 2010), and the following pulses mainly reflect release of newly-replenished SVs at release sites. The capacitance decay was fitted by a dual exponential. $Cm = C_{fast} \exp(-x/\tau_1) + C_{slow} \exp(-x/\tau_2)$. It was fitted with two time constants of a few seconds ($\tau = 5.2$ s, $C_{fast} = 37$ %) and tens of seconds ($\tau = 66.5$ s, $C_{slow} = 63$ %), reflecting clathrin-independent and dependent endocytosis, respectively (Wu et al., 2009; Yamashita et al., 2010). During the recording, we also measured the fluorescence of the cypHer signal. The cypHer fluorescence showed a rapid decrease upon stimulation, followed by a slow recovery (Figure 9D). The time course of fluorescence change reflects the kinetics of exocytosis and subsequent endocytosis of Syt2, in addition to re-acidification of endocytosed vesicles. To compare the time course of membrane capacitance traces and cypHer fluorescence traces, I inverted the cypHer traces. Comparison of the recovery time course of the capacitance traces and the cypHer traces showed that both returned to ~0.4 of the peak value after 60 s (C_m, 0.33 ± 0.06, n =7; F, 0.47 ± 0.07, n = 10, Figure 9E). Two notable features are revealed by comparing capacitance and cypHer measurements: (1) C_m

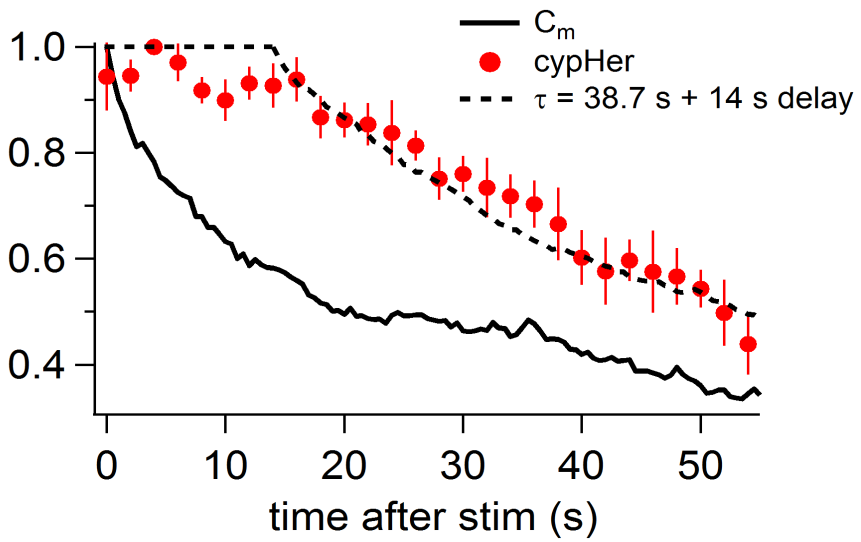

Figure 11. Comparison of the recovery time course of capacitance and cypHer (rat)
By assuming a certain delay and a re-acidification time constant of the endocytosed organelle after membrane retrieval, the recovery time course of cypHer signal (red circles) was fitted. The re-acidification time course of the endocytosed organelle was assumed to be an exponential from pH7.4 to pH5.5. The fitting curve is convolution of the Cm time course (bold line) with best fit delay and re-acidification time constant, calculated by least squares method. During the delay, the value was held to be 1. The cypHer signal was best fitted if one assumes that a 14 s delay with a 38.7 s re-acidification time constant after membrane retrieval (dotted line).

had a rapid decay component whereas cypHer signals did not (see also Figure 11 below); (2) CypHer signals showed a delay in the decay phase as compared with the decay of the capacitance values. The slower recovery of cypHer signal compared with capacitance is consistent with reports showing that acidification of glutamatergic SVs occurs with a time constant of tens of seconds (Egashira et al., 2015 but see Atluri and Ryan, 2006). CypHer signals have a delay of 10-20 s and an exponential decay with a time constant of tens of seconds (Fig 11, 12), and I fitted the recovery as following. (1) I assumed that capacitance traces reflect endocytosis of membrane. (2) I assumed that each endocytosed vesicle is acidified exponentially with a fixed time constant. (3) Following the pH dependence of cypHer signals (Hua et al., 2011), cypHer fluorescence changes. For each 0.5 s, the number of endocytosed vesicles was estimated based on capacitance measurements, and these vesicles were acidified with the acidification time constant. Time course of acidification was then converted to fluorescence change. Therefore, the fit was the convolution of endocytosis of membrane, acidification time course and pH-dependence of cypHer fluorescence. The experimental data could not be fitted without a delay of 14 s of onset after membrane retrieval for each endocytosed vesicle. Fitting of the recovery time course of the cypHer signal was optimal with a re-acidification time

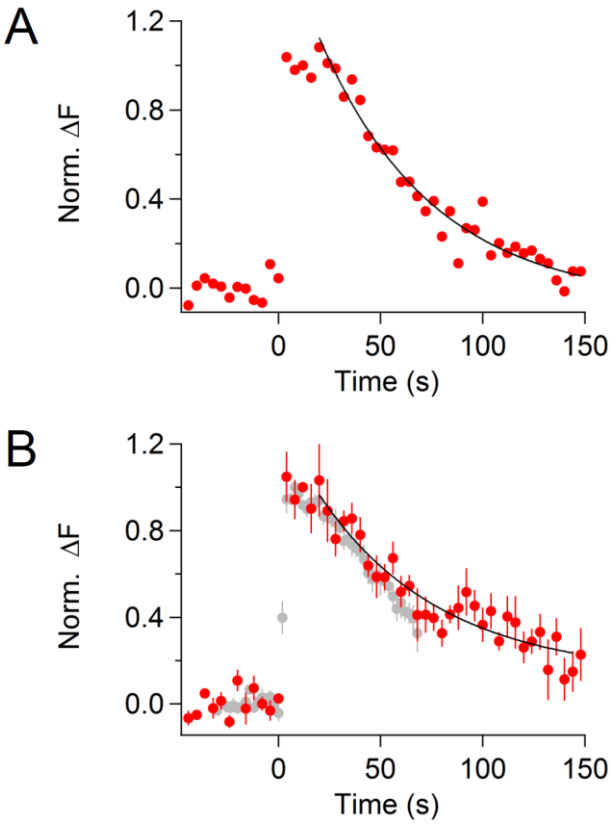

Figure 12. CypHer signal recovery after a train of depolarizing pulses (longer recording)
(A) An example trace of cypHer signal recovery after a train of depolarization (see Figure 9C) is shown for a longer recording period. To avoid bleaching of cypHer, the frequency of image acquisition was reduced to every 4 s. The cypHer signal recovery was best fitted with an exponential ($F = \Delta F \exp(-x/\tau)$; $\tau = 55.5$ s) with a 16 s delay.
(B) Averaged trace of cypHer signal recovery for a longer recording period (red circles, n = 5). The averaged cypHer signal recovery was best fitted with an exponential ($\tau = 59.7$ s) with a 16 s delay. Gray circles are averaged cypHer signal from shorter recordings, same trace as shown in Figure 9E (bottom).

constant of 38.7 s (Figure 11). The reason for the delay is unclear, but given that membrane retrieval is proceeding continuously after stimulation, it is likely that newly-endcytosed vesicles, and particularly endosome -like vesicles that contribute to the fast phase of endocytosis (bulk endocytosis) are not acidified or acidified very slowly for 10-20 seconds. It should be note that this is a rough estimation and that re-acidification time constant of vesicles and pH dependence of the cypHer kinetics should be measured independently (Atluri and Ryan, 2006; Egashira et al., 2015), if one wants to estimate the rate of retrieval of Syt2 accurately. In addition, because endocytosis is slow and the amounts of exo/endocytosis are large (> 10000 vesicles), the time course of fluorescence change is determined by endocytosis rather than acidification. Therefore, I cannot estimate the exact time course of Syt2 retrieval rigidly though most likely Syt2 retrieval should be faster than fluorescence changes. The asymptotic value (extrapolated from the exponential fit) of the fluorescence recovery (0.13 from Figure 12) was similar to that of the capacitance trace (0.12 from Figure 9E), which indicated that the rate of endocytosis becomes as low as that of re-acidification. The exponential decay time constant was more clearly seen by taking longer recording (Figure 12), suggesting that exocytosed Syt2 is almost retrieved (> 80 %). There may be some incomplete retrieval, or photo-bleaching of cypHer signals.

To investigate the time course of Syt2 retrieval upon exo-endocytosis using anti-Syt2-cypHer, I have to assume that anti-Syt2-cypHer labeling of the vesicles is homogenous within my resolution and stimulus conditions. I cannot exclude the possibility that there is some heterogeneity in more subtle level. To verify this, I compared the magnitude of the capacitance jumps with the amplitude of cypHer fluorescence to see whether they correlate linearly. I applied four consecutive 50 ms depolarizing pulses with 20 s intervals, and simultaneously measured the size of the capacitance jumps and the cypHer fluorescence change. With this protocol, capacitance jumps showed a gradual decrease because of incomplete recovery of the readily releasable vesicle pool between the stimuli (Figure 13A). The amplitudes of the cypHer signal also showed gradual decrease (Figure 13B). When the normalized amplitudes of capacitance jumps and fluorescence decrease were compared, I found similar levels of depression (Figure 13C, D). This result indicates that the membrane capacitance

changes and the changes in cypHer fluorescence amplitudes correlate linearly, even under conditions of a slight change in the extent of exocytosis (~ 20 %), and that the cypHer labeling of the vesicles is homogenous in my resolution of the measurements.

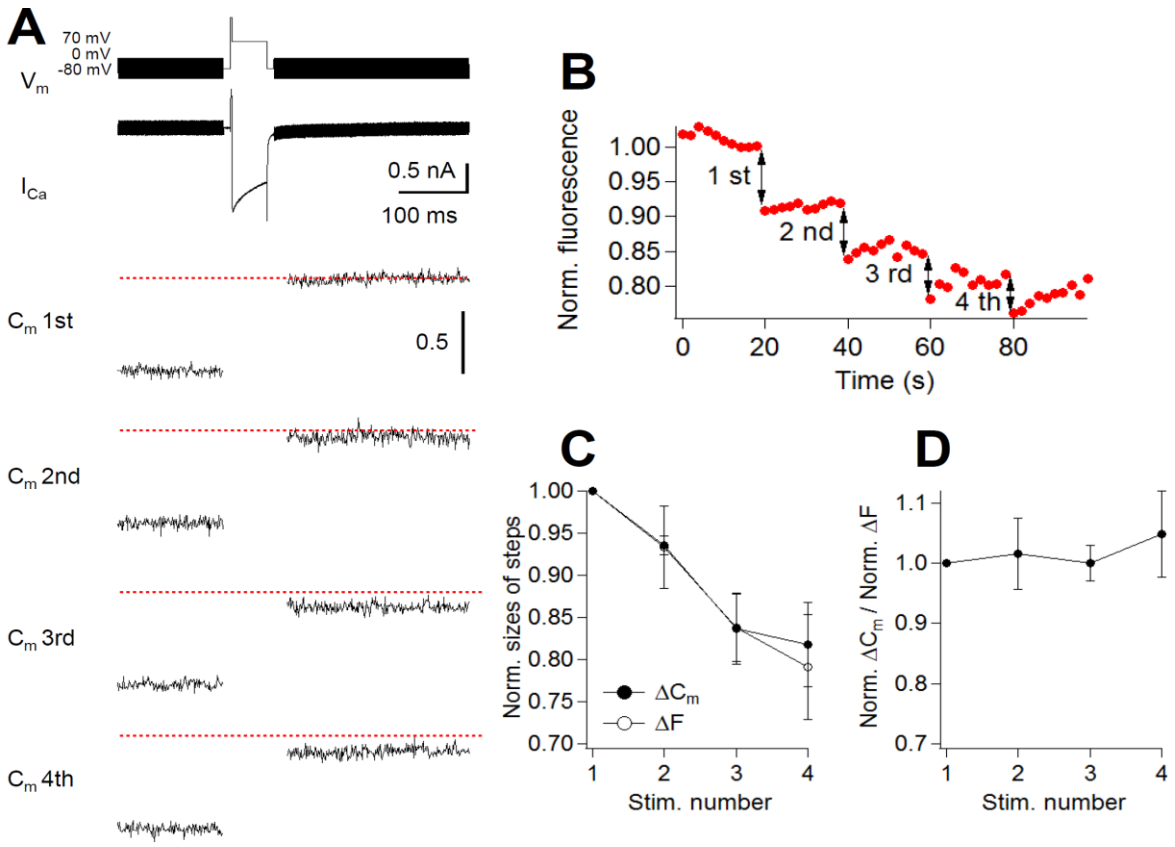

Figure 13. Correlation between the amount of membrane capacitance changes and cypHer signal changes

(A) A 50 ms depolarizing pulse (0 mV for 50 ms, following a prepulse to +70 mV for 2 ms), as shown on the top, was applied four times with an inter stimulus interval of 20 s. The bottom panels show averaged capacitance traces of four consecutive stimulations (n = 6). Traces from each cell were normalized to the first ΔC_m amplitude. The dotted red lines show the first ΔC_m amplitudes.
(B) Example of cypHer fluorescence changes induced by four consecutive 50 ms depolarizations.
(C) The extent of capacitance jumps (filled circles) and cypHer fluorescence changes (open circles) evoked by four consecutive depolarizations.
(D) The ratio of normalized ΔC_m and normalized ΔF of the cypHer signals plotted against the stimulus number.

Next, I examined if the recovery of the cypHer signal is caused by endocytosis and subsequent re-acidification. For this purpose, I blocked endocytosis and re-acidification by using pharmacological tools.

First, I inhibited endocytosis by applying dynamin inhibitory peptide (1 mM) intracellularly through the patch pipette. Dynamin is essential for slow endocytosis at the calyx terminal (Yamashita et al., 2005, 2010; Wu et al., 2009). After a 4-5 min waiting period to allow the peptide to diffuse throughout the terminal, I applied a train of ten 50 ms depolarizations. Dynamin inhibitory peptide inhibited endocytosis following a capacitance jump except for the early fast component (Figure 14A), which is consistent with previous reports (Yamashita et al., 2010), and the cypHer signal recovery was also blocked by dynamin inhibitory peptide (Figure 14A). Both the capacitance and the cypHer signal recovery were significantly slower in the presence of dynamin inhibitory peptide than under control conditions (Figure 14B). Normalized C_m after 60 s was 0.33 ± 0.06 for control calyces (n = 7), and 0.61 ± 0.05 in calyces treated with dynamin inhibitory peptide (n = 4, $p < 0.01$), while the cypHer signal recovered to a value of 0.47 ± 0.07 in control (n = 10) and to 0.92 ± 0.10 in the presence of dynamin inhibitory peptide (n = 4, $p < 0.01$).

Next, I blocked the re-acidification of endocytosed vesicles by bath application of bafilomycin, a V-type ATPase inhibitor (5 μM). I applied bafilomycin for 4-5 min before the recordings to block re-acidification of newly endocytosed vesicles. Upon application of a train of ten 50 ms depolarizations, capacitance showed a robust jump and a clear recovery after the jump, indicating that membrane retrieval was still functional in the presence of bafilomycin (Figure 14C). On the other hand, the cypHer signal did not recover, as expected under blockade of re-acidification by bafilomycin (Figure 14C; Sankaranarayanan and Ryan, 2001). Average traces (Figure 14D) showed no difference in the time course of capacitance recovery (normalized C_m after 60 s; control, 0.33 ± 0.06, n = 7; bafilomycin, 0.47 ± 0.08, n = 5, $p = 0.19$), but the recovery of cypHer signal was blocked with bafilomycin (normalized ΔF after 60 s; control, 0.47 ± 0.10, n = 10; bafilomycin, 1.22 ± 0.24, n = 5, $p = 0.03$). Although bafilomycin may directly block retrieval of syt2, more likely explanation is that bafilomycin blocks acidification of endocytosed SVs.

Based on these results, I conclude that the cypHer signal recovery results from endocytosis and subsequent re-acidification of the endocytosed organelles.

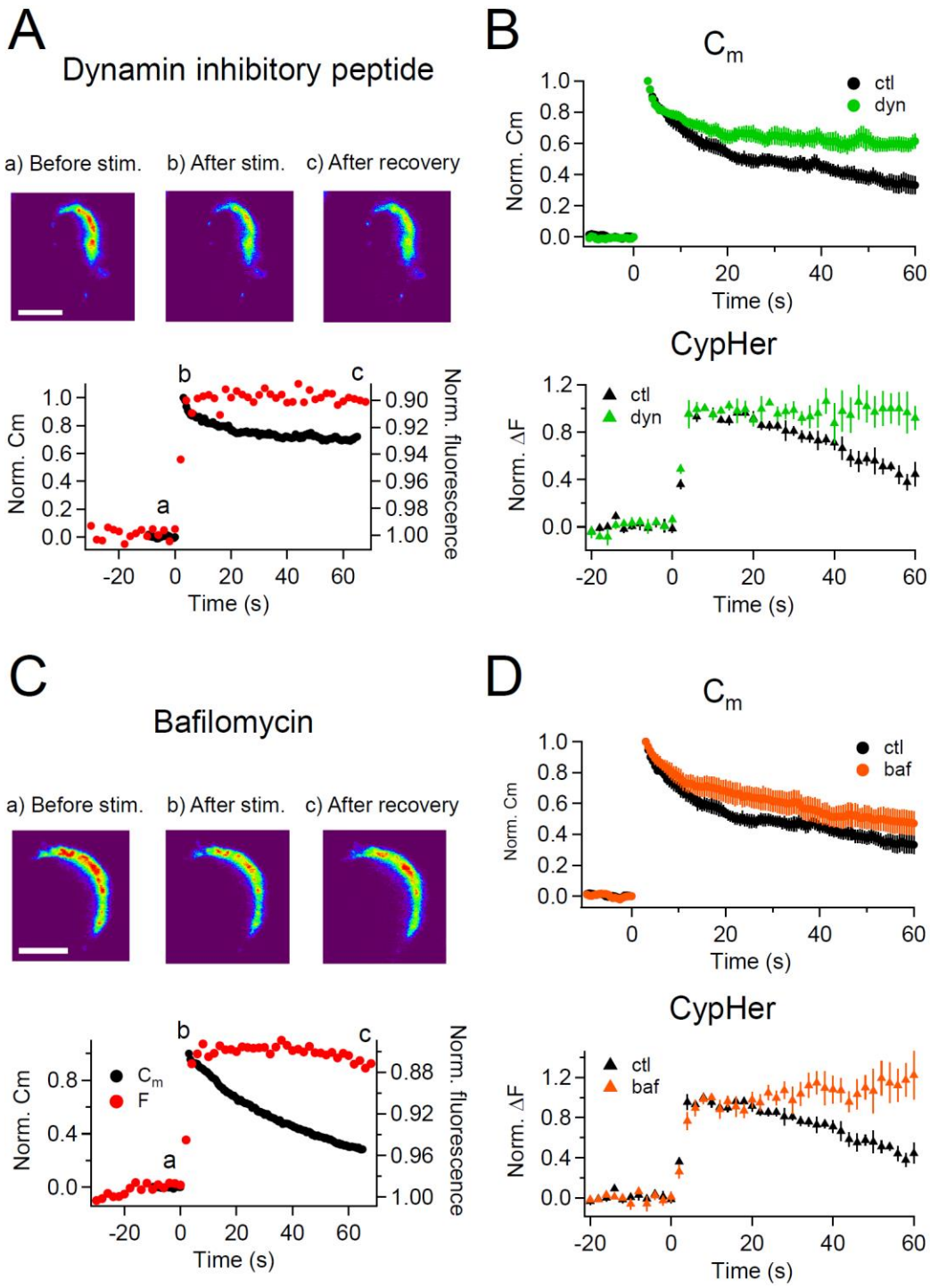

Figure 14. CypHer signal recovery depends on endocytosis and reacidification

(A) A train of depolarizing pulses (see Figure 9C) was applied to elicit exocytosis in the presence of 1 mM dynamin inhibitory peoptide. Images in the top panel show the cypHer fluorescence at the time point indicated in the plot below (see also Figure 9B). Scale bar, 10 µm. The bottom panel shows example traces of C_m and cypHer fluorescence in the presence of dynamin inhibitory peptide.

(B) The top panel shows averaged C_m traces under control conditions (n = 7, black circles) and in the presence of dynamin inhibitory peptide (n = 4, green circles). The bottom panel shows cypHer fluorescence changes under control conditions (n = 10, black triangles) and in the presence of dynamin inhibitory peptide (n = 4, green triangles). *Figure 14 continued on next page*

Figure 14 continued

(C) Same as in A, with 5 μM bafilomycin applied during the recording.

(D) The top panel shows averaged C_m traces under control conditions (n = 7, black circles) and in the presence of bafilomycin (n = 5, orange circles). The bottom panel shows averaged fluorescence traces under control conditions (n = 10, black triangles) and in the presence of bafilomycin (n = 5, orange triangles).

3.2. Syt2 is taken up into slowly re-acidifying organelles after prolonged depolarization

Because the fast and the slow components of endocytosis were co-detected with the capacitance measurements (Figure 9E), while the fast mode was not seen in the cypHer measurements (Figure 9B), I next examined more specifically the retrieval of Syt2 during fast endocytosis.

The fast mode of endocytosis occurs predominantly in response to strong stimulation in P8-11 calyx terminals, and is thought to be triggered by elevation of the bulk cytoplasmic Ca^{2+} concentration (Wu et al., 2005). This mode of endocytosis retrieves the plasma membrane extremely fast, which can be read out as a rapid membrane capacitance decay after the exocytotic capacitance jump, and often shows an undershoot (Renden and von Gersdorff, 2007; Wu et al., 2009). It has been shown that the amount of fast mode of endocytosis was gradually increased by elongating pulse durations in P8-11 calyx of Held terminals (Renden and von Gersdorff, 2007; Wu et al., 2009; Yamashita et al., 2010; Midorikawa et al., 2014). While the kinetics of this membrane retrieval has been characterized, the kinetics of the accompanying protein retrieval is largely unknown.

In this set of experiments, the calyx terminal was stimulated by a 2 s depolarization pulse to induce only a fast mode of endocytosis (Yao and Sakaba, 2012). The membrane capacitance showed a large jump upon the stimulation (> 1 pF, Figure 15A, left), and decayed rapidly after the stimulation,

which is consistent with previous studies. This fast mode of endocytosis is shown to be insensitive to dynamin inhibition (Yamashita et al., 2010; but see Xue et al., 2008), as fast component in Figure 14, suggesting the same mechanism. On the contrary, the cypHer signal barely showed a recovery (Figure

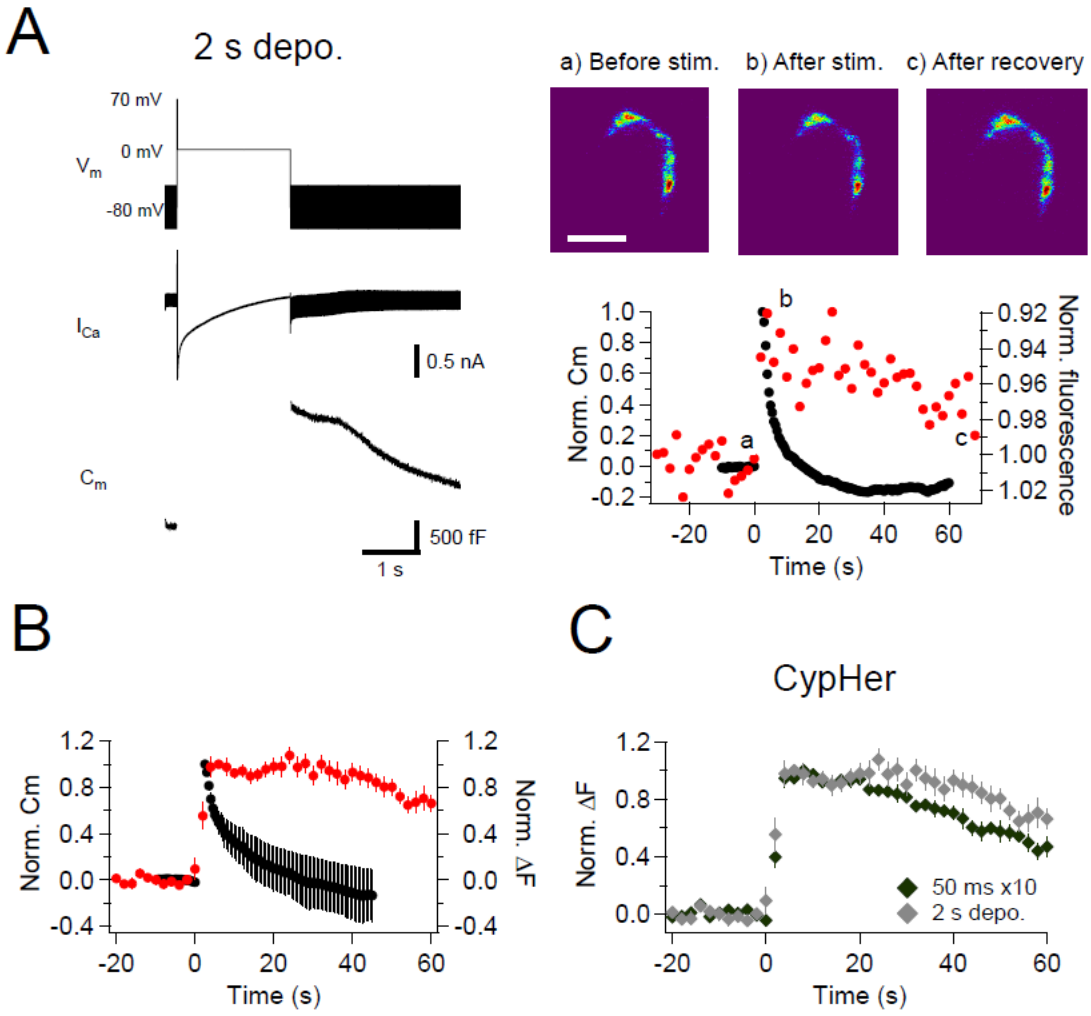

Figure 15. Effect of a prolonged depolarizing pulse on the kinetics of capacitance and cypHer signal recovery

(A) Similar to Figure 9, but a single prolonged (2 s) depolarization (V_m) was applied, which induced large calcium currents (I_{Ca}) and capacitance jumps (C_m). Images (right top) show the cypHer fluorescence at each time point shown in the panel below. Scale bar, 10 µm. The right bottom panel shows example traces of C_m and cypHer fluorescence obtained with the 2 s depolarization paradigm.

(B) Average traces of C_m (black circles) and cypHer fluorescence (red circles) at the calyx terminal evoked by a 2 s depolarizing pulse (n = 7).

(C) Averaged cypHer fluorescence traces obtained by applying a train of depolarizing pulses (the same as Figure 9C, n = 10, black diamonds) or by a 2 s depolarizing pulse (n = 7, gray diamonds). CypHer fluorescence recovery was slower after a 2 s depolarization (40 s after the stimulus; 50 ms x 10, 0.70 ± 0.04; 2 s, 0.93 ± 0.07, p = 0.019).

15A, right). The discrepancy was more clearly seen when I compared the averaged traces of membrane capacitance and cypHer signal (Figure 15B). This is different from the results obtained with trains of ten 50 ms depolarizations (Figure 9), where membrane capacitance and cypHer signal

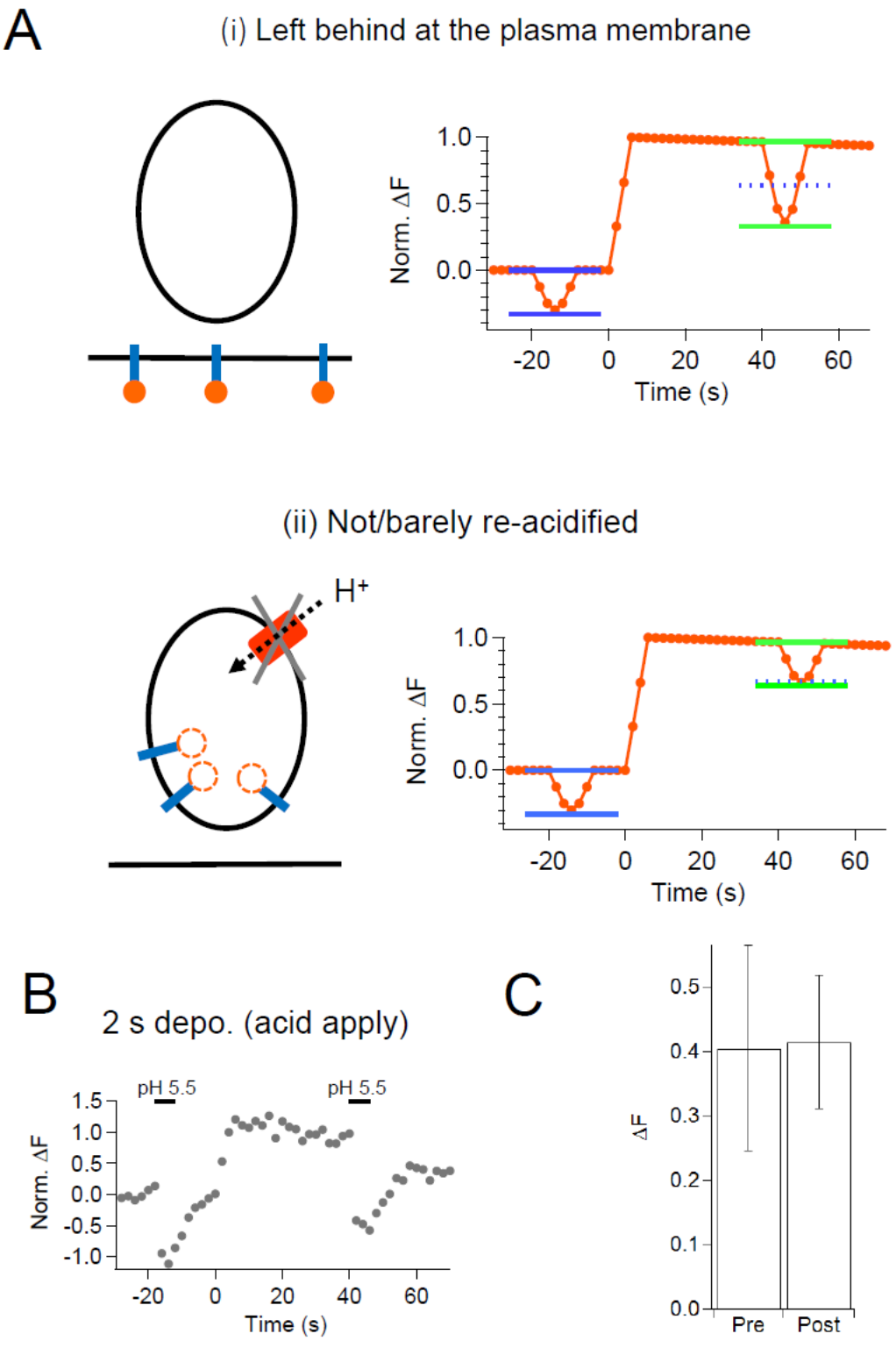

Figure 16. The kinetics of cypHer signal by a puff-application of an acidic (pH 5.5) solution on a prolonged depolarizing pulse

(A) Schematic views of the experiment of a puff-application. An acidic solution (pH 5.5) was briefly (5 s) applied extracellularly before (20 s) and after (40 s) the stimulation to de-quench the surface-exposed anti-Syt2-cypHer. **(i)** If the anti-Syt2-cypHer (orange dots) was left behind at the plasma membrane, the amount of de-quenching after stimulation (green line) should be higher than that of before stimulation (blue solid and dotted line)**. (ii)** If the anti-Syt2-cypHer (orange dots) was retrieved together with the plasma membrane and the endocytosed organelle was not/barely re-acidified, there should be no difference in the amount of de-quenching before and after stimulation.

(B) Example trace of cypHer fluorescence change when an acidic extracellular solution (pH 5.5) was puff-applied during the recording. The pH 5.5 solution was puff-applied twice for 5 s, 20 s before and 40 s after stimulation.

(C) Comparison of ΔF induced by the puff-application of pH 5.5 solution before (Pre) and after (Post) stimulation. There was no significant difference (Pre, 0.40 ± 0.16; Post, 0.41 ± 0.10, n = 5, p = 0.66).

decayed with more similar time courses. In fact, the recovery time course of cypHer signal after the 2 s depolarization was even slower than after trains of ten 50 ms depolarizations (Figure 15C, 40s after the stimulus; 50 ms x 10, 0.70 ± 0.04, n = 10; 2 s, 0.93 ± 0.07, n = 9, p = 0.019). To explain the delayed cypHer signal recovery after the 2 s depolarization condition, I considered two possibilities: (i) the anti-Syt2-cypHer was not retrieved together with the endocytosed membrane and left behind at the plasma membrane surface, or (ii) the anti-Syt2-cypHer was retrieved via endocytosed organelles, but the organelle lumen was not (or barely) re-acidified after endocytosis. To discriminate between these two possibilities, I briefly (5 s) applied an acidic solution (pH 5.5) extracellularly before (20 s) and after (40 s) the stimulation to de-quench the surface-exposed anti-Syt2-cypHer (Fig 16). In the 2 s pulse condition, membrane retrieval assessed by capacitance measurements is essentially completed 40 s after the stimulation. If the anti-Syt2-cypHer were taken up into the endocytosed organelle, there should be no difference in the amount of de-quenching before and after the stimulation. On the other hand, the amount of de-quenching should be higher after stimulation if anti-Syt2-cypHer were not taken up and left behind at the plasma membrane. I found (Figure 16B and C) that the amount of de-quenching was not different before or after the stimulation (pre, 0.37 ± 0.14; post, 0.40 ± 0.11, n = 5, p = 0.66), indicating that anti-Syt2-cypHer was retrieved via

endocytosed organelles, but the endocytosed organelles were not (or barely) re-acidified. The lack of re-acidification in the newly endocytosed organelles after a 2 s depolarization can be explained if the membrane endocytosis occurred as bulk endocytosis, which is seen after strong stimulation of the calyx terminal (de Lange et al., 2003). Longer post-stimulus recordings showed a sign of cypHer signal recovery (Figure 17), which is consistent with the idea that anti-Syt2-cypHer is initially taken up via larger endosomal-like structure formed by fast endocytosis, followed by slow re-acidification due to the larger volume-to-surface ratio.

Based on these results, I conclude that membrane and anti-Syt2-cypHer was retrieved together via endosome-like structure, though cypHer cannot measure the fast mode of endocytosis.

Given the results in Figure 14-17, the delay phase of cypHer signal recovery (Figure 9) was due to at least two reasons: (1) While membrane capacitance decrease reflects membrane retrieval itself, cypHer signal recovery depends on endocytosis and subsequent re-acidification (Figure 14), so that the recovery of cypHer signal may be slower than membrane capacitance decrease. (2) cypHer cannot measure fast endocytosis likely due to slow re-acidification of endosome-like structure (Figure

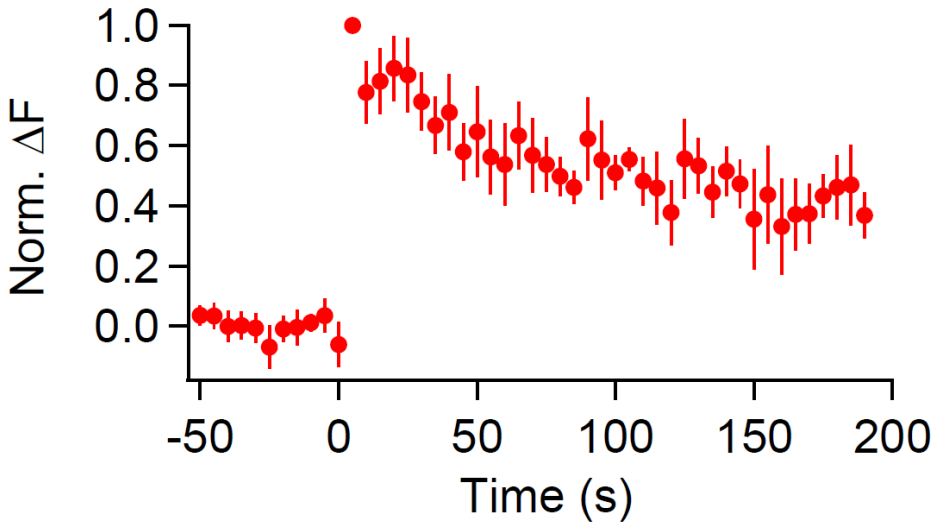

Figure 17. CypHer signal recovery after a prolonged depolarizing pulse (longer recording) The time course of cypHer signal recovery after a 2 s depolarization (see Figure 12A) is shown for a longer recording period. To avoid bleaching of cypHer, the frequency of image acquisition was reduced to every 5 s. The cypHer signal recovered to 0.36 ± 0.08 after 190 s (n = 4), similar to 60 s after train stimulation with ten 50 ms depolarizations (0.47 ± 0.07, n = 10). The time constant of recovery was difficult to estimate because the fluorescence does not recover to baseline, but from the initial slope of decay, the time constant of recovery was 150.4 s with no delay and 210.9 s with a 30 s delay. $F = \Delta F \exp(-x/\tau)$.

15 and 16). A train of depolarization pulses induced both fast and slow endocytosis (Figure 9), so that endosome-like structure may contribute to the delay phase of cypHer signal recovery (Figure 11). Thus, the recovery of cypHer signal may be convolution of three parameters (membrane retrieval, delay of re-acidification, and re-acidification).

3.3. Effect of calmodulin blockade on the coordinated retrieval of vesicular membrane and Syt2

It was suggested that CaM is crucial for clearing fused vesicle membrane and proteins from release sites (Wu et al., 2009; Hosoi et al., 2009). If so, then block of CaM should impair retrieval of SV proteins (see Introduction). To test the role of CaM in membrane and Syt2 retrieval during the slow

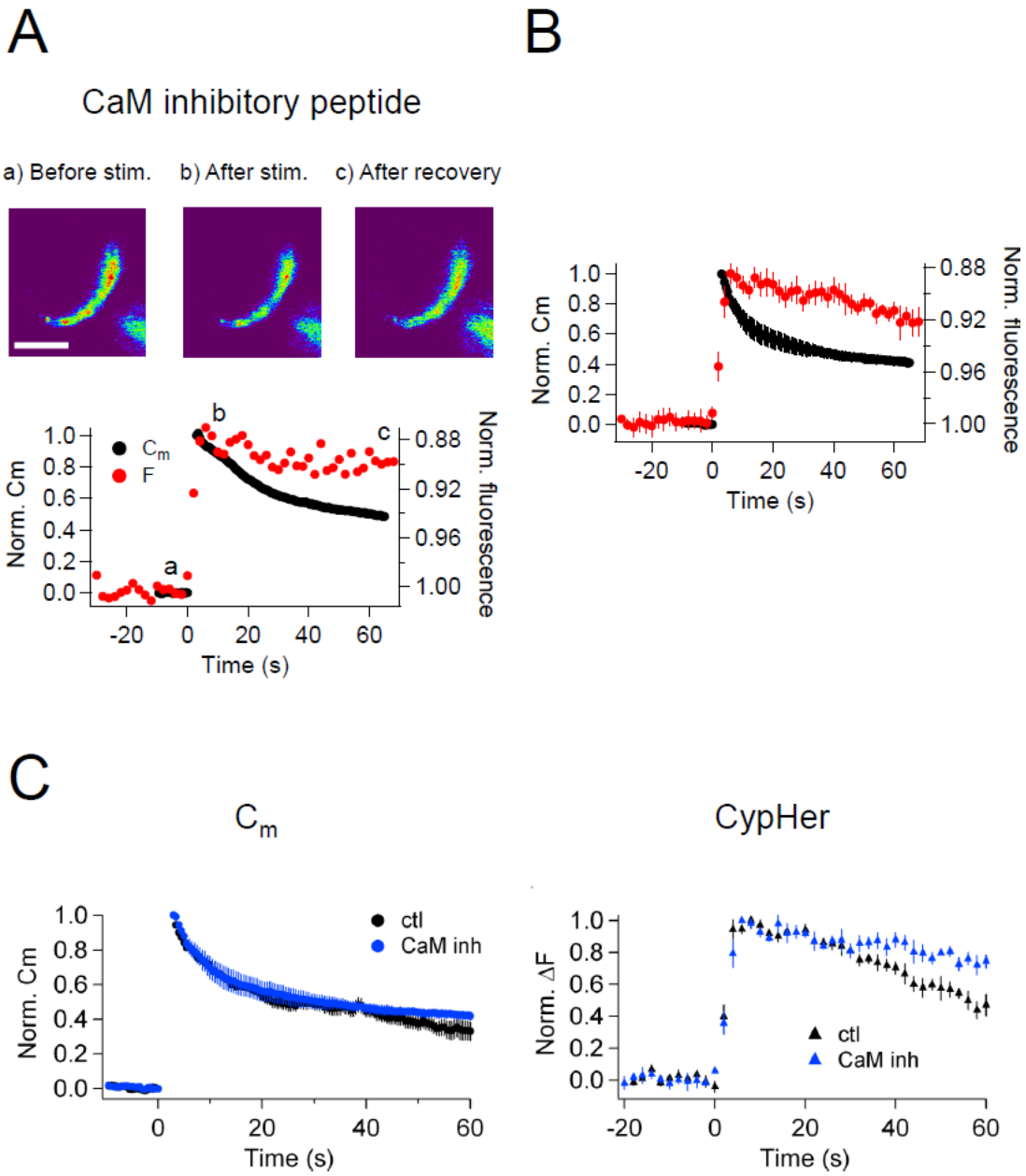

Figure 18. Effect of calmodulin inhibitory peptide on the kinetics of capacitance and cypHer signal recovery

(A) A train of depolarizing pulses (the same as Figure 9C) was applied to elicit exocytosis in the presence of 20 μM CaM inhibitory peptide. Images (top) show the cypHer fluorescence at each time point depicted in the bottom panel. The bottom panel shows example traces of C_m and cypHer fluorescence in the presence of the CaM inhibitory peptide. Scale bar, 10 μm.

(B) Average traces of C_m (black circles) and cypHer fluorescence (red circles) in the presence of CaM inhibitory peptide (n = 5).

(C) The left panel shows averaged C_m traces under control conditions (n = 7, black circles) and in the presence of CaM inhibitory peptide (n = 5, blue circles). The right panel shows averaged cypHer fluorescence traces under control conditions (n = 10, black triangles) and in the presence of CaM inhibitory peptide (n = 5, blue triangles).

mode of endocytosis, I inhibited CaM function by intracellular application of a CaM inhibitory peptide (20 μM). I particularly examined the condition of slow endocytosis, because it is known to be more relevant for synaptic vesicle replenishment (Hosoi et al., 2009), I have not studied the role of CaM in fast endocytosis. I whole-cell voltage clamped the calyx terminal and waited for 4-5 min to allow the peptide to diffuse into the terminal. Then, a train of ten 50 ms depolarizations was applied to evoke exocytosis followed by endocytosis, and the effects on membrane capacitance and cypHer signal recovery were monitored. In this protocol slow mode of endocytosis is dominant under control condition.

After the stimulus, membrane capacitance recovered, but the cypHer signal barely showed any recovery (Figure 18A, B). Averaged traces show that the time course of membrane retrieval was not affected (Figure 18C left, 60 s after the stimulus; control, 0.33 ± 0.06, n = 7; CaM inhibitory peptide, 0.42 ± 0.03, n = 5, p = 0.21), but the cypHer signal recovery was reduced and/or slowed down by application of CaM inhibitory peptide (Figure 18C right, 60 s after the stimulus; control, 0.47 ± 0.07, n = 10; CaM inhibitory peptide, 0.74 ± 0.04, n = 5, $p < 0.01$). It remains possible that a higher concentration of CaM inhibitor is required to inhibit membrane retrieval itself (Sun et al., 2010; Wu et al., 2014). To test if the slower recovery of the cypHer signal was caused by slower protein retrieval or else by slower re-acidification, I performed an acidic solution (pH 5.5) experiment as in Figure 16. I applied acidic solution before (20 s) and after (40 s) the train of ten 50 ms

depolarizations under control conditions in the absence (Figure 19A) or presence of CaM inhibitory peptide (Figure 19B). The amounts of de-quenching induced by acid perfusions, before and after stimulation, were measured in both conditions (Figure 19A, B). Then, I calculated the de-quenching ratio after and before the stimulation (post ΔF / pre ΔF), and compared the values between the two conditions. I found that the post ΔF / pre ΔF value was larger in the presence of CaM inhibitory peptide (control, 1.15 ± 0.20, n = 5; CaM inhibitory peptide, 1.95 ± 0.14, n = 5, p = 0.012, Figure 19C). The small increase in the post ΔF / pre ΔF ratio under control condition is caused by incomplete membrane retrieval 40 s after the stimulus (Figure 9). Because the time course of membrane retrieval was similar for both control and CaM inhibitory peptide conditions (Figure 18C), this result indicates that anti-Syt2-cypHer was left behind at the plasma membrane surface in the presence of CaM inhibitory peptide. Thus, CaM may play a crucial role in coordinated retrieval of Syt2 together with the endocytosed membrane. The data do not prove, but are consistent with the view that CaM

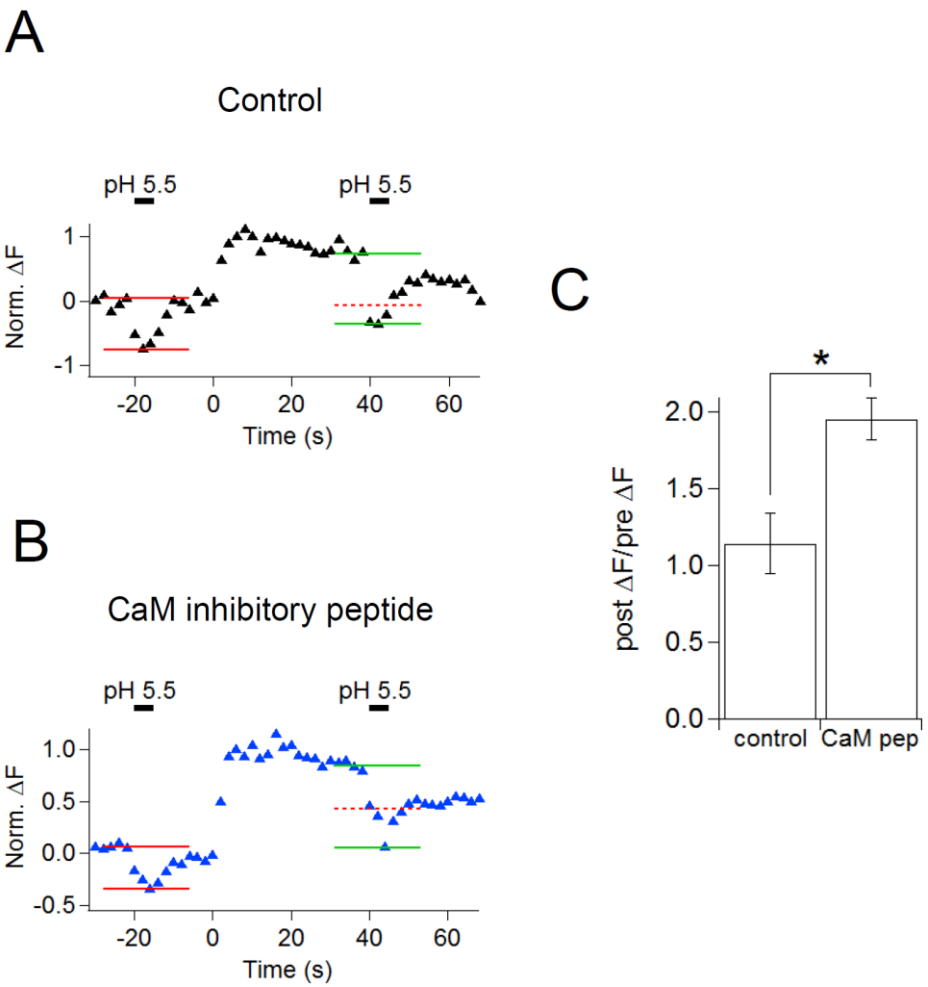

Figure 19. Effect of calmodulin inhibitory peptide on cypHer fluorescence changes induced by acidic solution application

(A) An example trace of the cypHer fluorescence change when an acidic extracellular solution (pH 5.5) was puff-applied during the recording without CaM inhibitory peptide. The pH 5.5 solution was puff applied for 5 s, once 20 s before and once 40 s after stimulation (50 ms pulse x 10). Red and green lines show the amount of fluorescence change induced by the pH 5.5 solution before and after stimulation, respectively. The dotted red line shows the amplitude of the 'before' signal.

(B) The same as A, but in the presence of 20 μM CaM inhibitory peptide.

(C) The de-quenching ratio before and after the stimulus (post ΔF/pre ΔF value) was larger in the presence of CaM inhibitory peptide (control, 1.15 ± 0.20, n = 5; CaM inhibitory peptide, 1.95 ± 0.14, n = 5, p = 0.012).

regulates synaptic vesicle replenishment by clearing SV proteins from the release sites (see discussion).

I also calculated the relative density of 'stranded' Syt2 present at the surface membrane before stimulation and that of the vesicular Syt2, based on the control condition data. The basal capacitance of the calyx terminal before the stimulation was 18.87 ± 1.56 pF, and the exocytotic capacitance jump caused by stimulation was 1.52 ± 0.21 pF. When fluorescent change was normalized to the amount of quenching upon stimulation (this value is 1), the amount of de-quenching by acid perfusion before the stimulus was 0.48 ± 0.23. From these values, I calculated the amount of fluorescence per area. The normalized ΔF/pF was 0.026 ± 0. 012 for the surface stranded Syt2 (ΔF = the amount of de-quenching by acidic perfusion before the stimulus/pF = the basal capacitance of the calyx terminal), and 0.71 ± 0.09 for vesicular Syt2 (ΔF = the amount of quenching upon stimulation/pF = the exocytotic capacitance jump). Thus, the density of vesicular Syt2 is ~ 30 times higher than the stranded Syt2. This number is in line with previous reported value for Syt1 at synapses of cultured hippocampal neurons (Fernández-Alfonso et al., 2006; Wienisch and Klingauf, 2006).

3.4. Calmodulin-Munc13-1 signaling is crucial for regulating the coordinated retrieval of vesicular membrane and Syt2

The AZ protein Munc13-1 is an essential priming factor for exocytosis (Varoqueaux et al., 2002). The priming activity of Munc13s is regulated by three independent domains, one of which is a Ca^{2+}-CaM binding domain (Junge et al., 2004; Lipstein et al., 2012). Analyses of a knock-in (KI) mouse line that expresses a Ca^{2+}-CaM insensitive Munc13-1 variant (Munc13-1^{W464R}) instead of wild-type (WT) Munc13-1 (Munc13-1^{WT}) showed that the Ca^{2+}-CaM-Munc13-1 signaling pathway regulates the recovery rate of the releasable SV pool in the calyx of Held (Lipstein et al., 2013). Based on clearance hypothesis, I hypothesized that the Ca^{2+}-CaM-Munc13-1 pathway might be an important post-exocytosis molecular organizer and regulate SV replenishment, in addition to its classical role in vesicle priming. Since CaM inhibition slowed the time course of Syt2 retrieval, I considered the possibility of Munc13-1 acting as a downstream target of CaM in this scenario, and tested if retrieval of Syt2 was affected at calyx terminals of Munc13-1^{W464R} KI mice as compared to WT littermates.

I used trains of ten 50 ms depolarizations to evoke exocytosis, and measured the recovery time courses of membrane capacitance and cypHer fluorescence. Recordings from WT mouse calyx terminals showed that the time course of cypHer signal recovery was similar to that of membrane capacitance retrieval (Figure 20A). The time courses of capacitance and cypHer were essentially similar between mice and rats. Fits based on the assumption of re-acidification with an exponential time constant of 18.9 s after membrane retrieval and a 12 s delay of onset described the actual recovery of the cypHer signal very well (Figure 21). In contrast, recordings from Munc13-1^{W464R} KI mouse calyx terminals showed a slower time course of cypHer signal recovery than of the membrane retrieval in 6 out of 7 recordings (Figure 20B). Comparison of averaged traces showed that the time course of membrane retrieval was not different between WT and Munc13-1^{W464R} KI calyces (Figure 20C left, 56 s after the stimulus; Munc13-1^{WT}, 0.20 ± 0.05, n = 8; Munc13-1^{W464R}, 0.17 ± 0.04, n = 6, p = 0.62), but the cypHer signal recovery was significantly smaller in Munc13-1^{W464R} KI calyces as compared to WT calyces (Figure 20C right; Munc13-1^{WT}, 0.26 ± 0.04, n = 8; Munc13-1^{W464R}, 0.72 ± 0.13, n = 6, p = 0.015). Together with the finding that the blockade of CaM inhibits the co-retrieval of Syt2 and membrane (Figure 18, 19), this result indicates that the Ca^{2+}-CaM-Munc13-1 pathway is crucial for coordinated retrieval of Syt2 together with endocytosed

membrane, supporting the notion that Munc13-1 is a downstream effector of CaM during endocytotic vesicular protein retrieval.

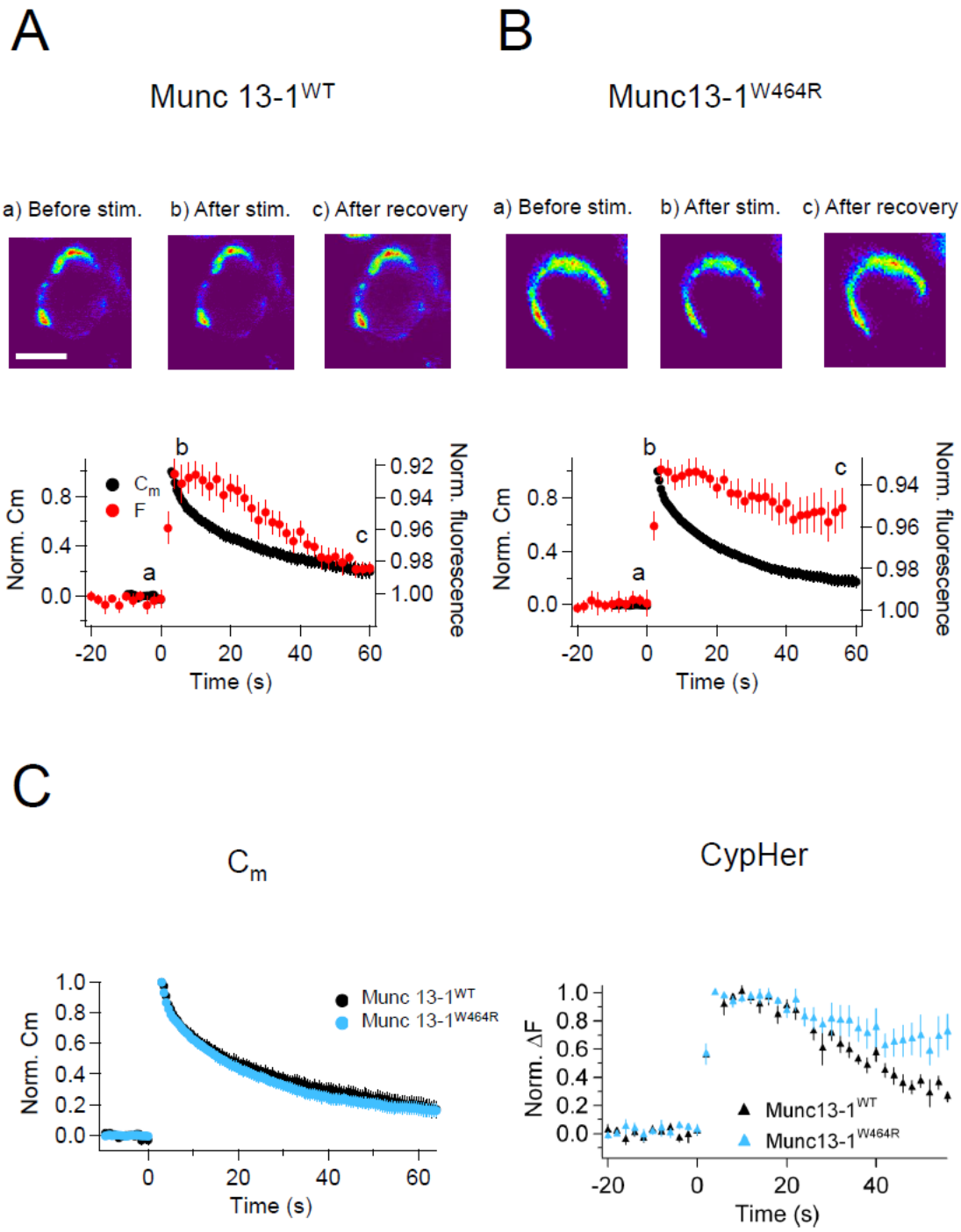

Figure 20. Capacitance and cypHer signal recovery in the calyx of Held of Munc13-1^{W464R} KI mice

(A) The same as Figure 9D and E, but recordings from calyx of Held terminals of wild-type (Munc13-1^{WT}) mice. The top panel shows the cypHer images at the time points shown in the bottom panel, and the bottom panel shows averaged C_m (black circles) and cypHer fluorescence (red circles) changes (n = 8). Scale bar, 10 µm. *Figure 20 continued on next page*

Figure 20 continued

(B) The same as A, but recordings from calyx of Held terminals of Munc 13-1^{W464R} mice (n = 6). Black and red traces show average normalized C_m and fluorescence changes. 3 out of 6 data were obtained from simultaneous measurements of capacitance and cypHer.

(C) The left panel shows averaged C_m traces from Munc13-1^{WT} calyces (n = 8, black circles) and Munc13-1^{W464R} calyces (n = 6, turquoise circles). The right panel shows averaged cypHer fluorescence traces from Munc13-1^{WT} calyces (n = 8, black triangles) and Munc13-1^{W464R} calyces (n = 6, turquoise blue triangles).

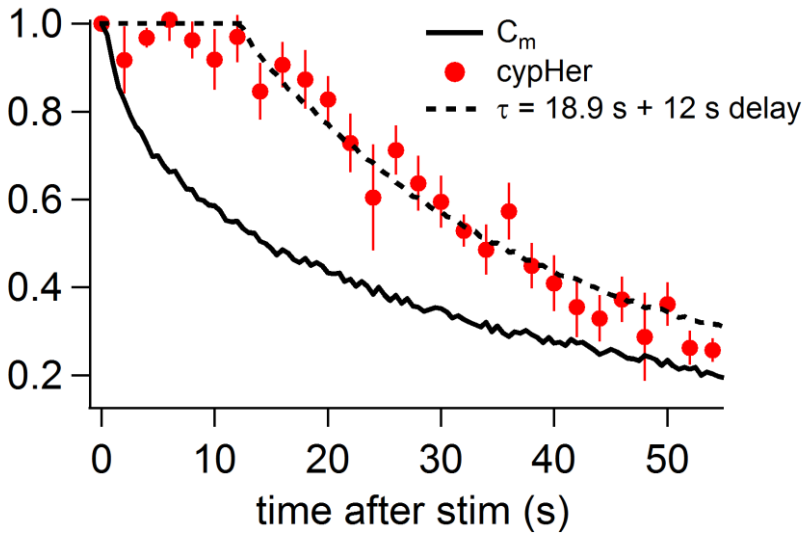

Figure 21. Comparison of the recovery time course of capacitance and cypHer (mouse)

By assuming a certain delay and a re-acidification time constant of the endocytosed organelle after membrane retrieval, the recovery time course of cypHer signal (red circles) was fitted. The re-acidification time course of the endocytosed organelle was assumed to be an exponential from pH7.4 to pH5.5. The fitting curve is convolution of the Cm time course (bold line) with best fit delay and re-acidification time constant, calculated by least squares method. During the delay, the value was held to be 1. The cypHer signal was best fitted with a 12 s delay with a 18.9 s re-acidification time constant after membrane retrieval (dotted line).

4. Discussion

Coordinated cycling of vesicle membrane and vesicle proteins is a critical process by which the pool of releasable SVs is repopulated to maintain synaptic transmission over extended periods of time. Owing to the large size of the calyx of Held presynaptic terminal, I was able to simultaneously measure the time course of membrane and vesicular protein (Syt2) retrieval in this synapse and made three key observations.

(1) The vesicle membrane retrieval, as assessed by capacitance measurements, and the Syt2 retrieval, as assessed by the fluorescence of the anti-synaptotagmin2-cypHer5E probe, had a similar time course when slow endocytosis was elicited (Figure 9).

(2) When fast endocytosis was elicited, Syt2 was still retrieved together with the membrane. However, acidification of the endocytosed organelles was very slow as determined by the divergence of the apparent recovery time courses of the membrane capacitance and the pH sensitive anti-synaptotagmin2-cypHer5E probe (Figure 15). This also suggests that pHluorin or related probes are not necessarily monitoring fast endocytosis faithfully.

(3) The simultaneous retrieval of membrane and Syt2 was disturbed by CaM inhibition (Figure 14), and the exocytosed Syt2 was left behind at the plasma membrane following membrane retrieval (Figure 15). In Munc13-1^{W464R} calyces a similar phenotype was seen, indicating that Ca^{2+}-CaM-Munc13-1 signaling, which is triggered by Ca^{2+} elevation during repetitive activity, might be crucial for regulating the coordinated retrieval of membrane and vesicular proteins (Figure 20).

On aggregate, these findings identify a signaling pathway that coordinates the retrieval of vesicle membrane and vesicle proteins, and that is regulated in a Ca^{2+}-CaM-Munc13-1-dependent manner. Also, I suggest that fast mode of endocytosis may not be monitored properly using pHluorin based probes.

4.1. Comparing the kinetics of vesicle membrane and vesicle protein retrieval

Several pH sensitive probes conjugated to vesicular proteins have been used to examine the kinetics of exo-endocytosis by taking advantage of the difference between intravesicular (~5.5) and extracellular (~7.4) pH. In many studies, it was assumed that the kinetics of the fluorescence changes represent endocytosis, including both, membrane and labeled protein retrieval. By directly comparing the kinetics of membrane and anti-Syt2-cypHer retrieval, I show here that this assumption is essentially correct at the calyx of Held presynaptic terminal when the stimulation intensity is mild. Under this condition, endocytosis is operated mainly by a slow, clathrin-dependent mode (Yamashita et al., 2010). The time course of cypHer signal recovery under this condition was slightly slower than that of the capacitance recovery, but the difference can be well described by taking the re-acidification time course (20 s ~ 40 s) into account. This is slightly longer than recent reports showing that the re-acidification time course of glutamatergic vesicles takes 15 seconds in cultured hippocampal neurons (Egashira et al., 2015). In some studies, even faster re-acidification time courses were suggested (Gandhi and Stevens, 2003; Atluri and Ryan, 2006). One of the possibilities that may cause the slow re-acidification time course was relatively large size of the synaptic vesicles in the calyx terminal (50 nm, Sätzler et al., 2002). These vesicles may contain up to 5000-7000 glutamate molecules. Recently, Cho and von Gersdorff (2014) reported that vesicular glutamate may function as a buffer for vesicle protons. So a larger vesicle may contain many hundreds to thousands of protons and its acidification may take a relatively long time. However, the time constant for single vesicle glutamate filling at the calyx of Held is estimated to be 15 seconds (Hori and Takahashi, 2012). In my train stimulation protocol, 37 % of membrane retrieval was mediated by fast endocytosis, thus larger endosome-like structure might also contribute to the slower re-acidification time course. Nicholson-Fish et al. (2015) have shown that bulk endocytosis at hippocampal culture was mediated by VAMP4 and that other synaptic vesicle proteins were excluded in the endocytosed vesicles. The bulk endocytosis I have seen at the calyx of Held is different, because syt2 is retrieved. In addition, they have not seen a delay in fluorescence change of VAMP4 fluorescence whereas I have seen a delay. The reason for the difference is unclear, but either what I have seen is different from Nicholson-Fish et al. or else it is possible that the endocytosed vesicles in this study are larger.

Previous reports employing pHluorin-based probes showed that endocytosis gets slower with stronger stimulation (Armbruster et al., 2013; Fernández-Alfonso and Ryan, 2004). Usually, clathrin-dependent, slow endocytosis is observed after mild stimulation, but in these pHluorin-based studies (Armbruster et al., 2013; Fernández-Alfonso and Ryan, 2004), endocytosis-based signal recovery was still slow (tens of seconds) even with strong stimulation, which elicits clathrin-independent endocytosis. In contrast, capacitance measurements and electron microscopic studies showed that clathrin-independent endocytosis, i.e. either bulk endocytosis or ultrafast endocytosis, occurs in the range of tens of ms to seconds (Jockusch et al., 2005; Wu et al., 2005; Watanabe et al., 2013). Fast endocytosis in the present study (Figure 15) reflects clathrin-independent endocytosis (de Lange et al., 2003), and by providing a direct comparison of membrane retrieval, vesicle protein retrieval, and re-acidification of endocytosed organelles, my results reconcile the previously reported, apparent discrepancy in the kinetics of endocytosis as assessed by pHluorin probes vs. capacitance measurements and electron microscopic analyses. My data demonstrate that the retrieval of vesicle membrane and vesicle proteins occurs simultaneously, but that re-acidification of the endocytosed organelle is slow after clathrin-independent, fast endocytosis. This is likely due to the large surface-to-volume ratio of the endosome-like structures that form during fast endocytosis and/or to slow budding of vesicles from such endosomes (Watanabe et al., 2014; Kononenko et al., 2014; Kononenko and Haucke, 2015)

4.2. The molecular basis of coordinated retrieval of vesicle membrane and vesicle proteins

In the present study, I examined the exo-endocytotic cycling of Syt2 using cypHer as a reporter. The lack of SV2 (Yao et al., 2010) or stonin2 (Kononenko et al., 2013) compromises the fidelity of synaptotagmin sorting, but the kinetics of clathrin-dependent slow endocytosis is unchanged even when synaptotagmin sorting is perturbed (Kononenko et al., 2013). This suggests that membrane retrieval and sorting of SV proteins can be segregated. My results are consistent with this notion, and the two processes can be separated in the presence of a CaM inhibitor or in Munc13-1^{W464R} calyces (Figure 18, 20). However, the possibility remains that several independent cycling pathways exist for

a given vesicle protein. For instance, VGLUT deficiency slows the recycling of synaptophysin but not of Syt1 (Pan et al., 2015), while stonin 2 deficiency slows the recycling of Syt1 but not of synaptophysin or synaptobrevin 2 (Kononenko et al., 2013).

CaM inhibitors and the perturbation of Ca^{2+}-CaM-Munc13-1 signaling perturb Syt2 retrieval without altering membrane retrieval kinetics (Figure 18, 20). However, calcineurin, a downstream target of CaM, was shown to be necessary for membrane retrieval (Sun et al., 2010; Wu et al., 2014). For three reasons, my results do not necessarily contradict these calcineurin data. First, it is possible that the complex between CaM and calcineurin is so tight that higher concentrations of CaM inhibitors are required to block the function of calcineurin in membrane retrieval. Second, the effect of CaM blockers on membrane retrieval can be seen when low concentrations of Ca^{2+} buffers are present in the presynaptic patch pipette, which lead to a strong elevation of the global presynaptic calcium concentration (Wu et al., 2014), but not when high concentrations of Ca^{2+} buffers are used as in the present study (see materials and methods in Section 2). Third, a CaM-independent component of membrane retrieval might exist. All this notwithstanding, my results suggest that CaM has several downstream targets that regulate the retrieval of membrane and proteins.

Clathrin-independent endocytosis, which forms large endosome-like structures by retrieving large pieces of membrane, has been observed at many types of synapses after strong stimulation (Thomas et al., 1994; Holt et al., 2003; Wu et al., 2009). Recent findings indicate that the plasma membrane adaptor AP-2 is required for vesicle regeneration from bulk endosome-like organelles in central nerve terminals (Kononenko et al., 2014; Watanabe et al., 2014), but it is not known how long it takes for vesicles to bud from the endosome-like organelles after bulk endocytosis. I found in this context that re-acidification barely occurs 1 min after a 2 s depolarization (Figure 15), which suggests that vesicle budding from endosome-like organelles is slow (Cheung et al., 2010). My results also suggest that Syt2 is retrieved together with the membrane not only in the slow, but also in the fast mode of endocytosis, but the molecular mechanism of Syt2 sorting during bulk endocytosis remains to be elucidated.

4.3. The role of CaM-Munc13 signaling in the coordinated retrieval of membrane and Syt2

I showed that CaM inhibition slowed down retrieval of Syt2 without affecting the kinetics of membrane retrieval (Figure 18, 19), and my data indicate that Munc13-1 is a possible downstream target of Ca^{2+}-CaM signaling in this process (Figure 20). This is somewhat surprising since Munc13-1 is a well-known vesicle priming factor at the AZ. In this context, the Ca^{2+}-CaM-Munc13-1 signaling pathway regulates the recovery rate of the pool of releasable SVs in hippocampal neurons (Junge et al., 2004; Lipstein et al., 2012) and in the calyx of Held terminal (Lipstein et al., 2013), likely by enhancing the replenishment rate of synaptic vesicles. However, the effect of dynamin inhibition, which perturbs endocytosis, on the SV replenishment rate (Wu et al., 2009; Hosoi et al., 2009) is very similar to the effect measured in the Munc13-1^{W464R} KI calyces (Figure 20), and to that of acute pharmacological blockade of CaM (Sakaba and Neher, 2001). Because the effects of perturbed endocytosis on vesicle pool recovery can be explained by delayed clearance of AZ release sites from the remains of molecular complexes formed by the preceding fusion (Hosoi et al., 2009; Kawasaki et al., 2000), or by impaired structural recovery after the preceding exocytosis (Wu et al., 2009) in addition to priming of synaptic vesicles (Midorikawa and Sakaba, 2015), and based on the results of my present study, I propose that the Ca^{2+}-CaM-Munc13 complex does not only act in the regulation of SV replenishment but is also involved in release site clearance. In other words, the data are consistent with the view that Ca^{2+}-CaM-Munc13 complex regulates clearance of release sites to endocytotic sites located at peri-AZ, which is required for retrieval of Syt2 together with membrane. The total amount of exocytosis evoked by a train of ten 50 ms stimuli was smaller in Munc13-1^{W464R} KI calyces as compared to WT controls (Munc13-1^{WT}, 1.48 ± 0.14 pF, n = 8; Munc13-1^{W464R}, 1.10 ± 0.10 pF, n = 6, $p < 0.05$), but the amount of exocytosis elicited by the first pulse in the train was not different (Munc13-1^{WT}, 351.9 ± 31.3 fF, n = 8; Munc13-1^{W464R}, 330.0 ± 35.8 fF, n = 6, p = 0.66), which is consistent with a previous study showing slower SV replenishment at release sites in Munc13-1^{W464R} KI calyces (Lipstein et al., 2013).

My finding that the retrieval of Syt2 is perturbed by CaM inhibition and in Munc13-1^{W464R} calyces supports the idea that Ca^{2+}-CaM-Munc13-1 signaling plays a role particularly in the retrieval

of Syt2. Disruption of exocytotic proteins such as SNAREs affects endocytosis, which suggests a close coupling between exo- and endocytotic processes (Hosoi et al., 2009; Zhang et al., 2013). Syt1 is needed for Ca-dependence of clathrin-mediated endocytosis in chromaffin cells (Yao et al., 2012; McAdam et al., 2015), and inhibition of Syt2 interaction to AP2 blocks clathrin-mediated endocytosis in calyx terminals (Hosoi et al., 2009). Also, genetic deletion of SV proteins perturbs endocytosis (Nicholson-Tomishima and Ryan, 2004; Deák et al., 2004). One possible molecular scenario is that the core complex of the release machinery, composed of SNAREs, Munc13s, Munc18s, and synaptotagmin (Betz et al., 1997; Ma et al., 2013), has to be disassembled before endocytosis, and that without a functional Ca^{2+}-CaM-Munc13-1 pathway, exocytosed Syt2 might be harder to dissociate from the release complex, so that Syt2 translocation to the endocytotic sites is retarded, causing a molecular jam at the AZ. It will be interesting to examine whether the retrieval of other proteins involved in the vesicle fusion complex are also regulated by Ca^{2+}-CaM-Munc13-1 signaling. On the other hand, it may be possible that CaM-Munc13-1 signaling is required for sorting of Syt2 to synaptic vesicles before endocytotic process (the step between clearance and endocytosis).

In any case, my results show that the coordinated endocytotic retrieval of membrane and proteins is subject to modulation by second messenger pathways, and thus is a potential target of modulation during presynaptic plasticity. This might be particularly relevant in the calyx of Held, which has to cope with high-frequency transmission (Taschenberger et al., 2002) and where Ca^{2+} elevation boosts proper SV sorting and replenishment, but other synapses may employ the same regulatory mechanism. So far, the calyx of Held terminal is the most convenient neuronal presynaptic terminal for capacitance measurements, but recently several other neuronal presynaptic terminals, where genetic manipulations are better feasible, were shown to be amenable to capacitance recordings (e.g. hippocampal mossy fiber terminals, Hallermann et al., 2003; cerebellar mossy fiber boutons, Delvendahl et al., 2015; cultured cerebellar Purkinje cell, Kawaguchi and Sakaba, 2015). Because endocytotic mechanisms may differ among synapse types (Kononenko and Haucke, 2015), it will be interesting to examine the differential kinetics of vesicular protein retrieval in these preparations as well.

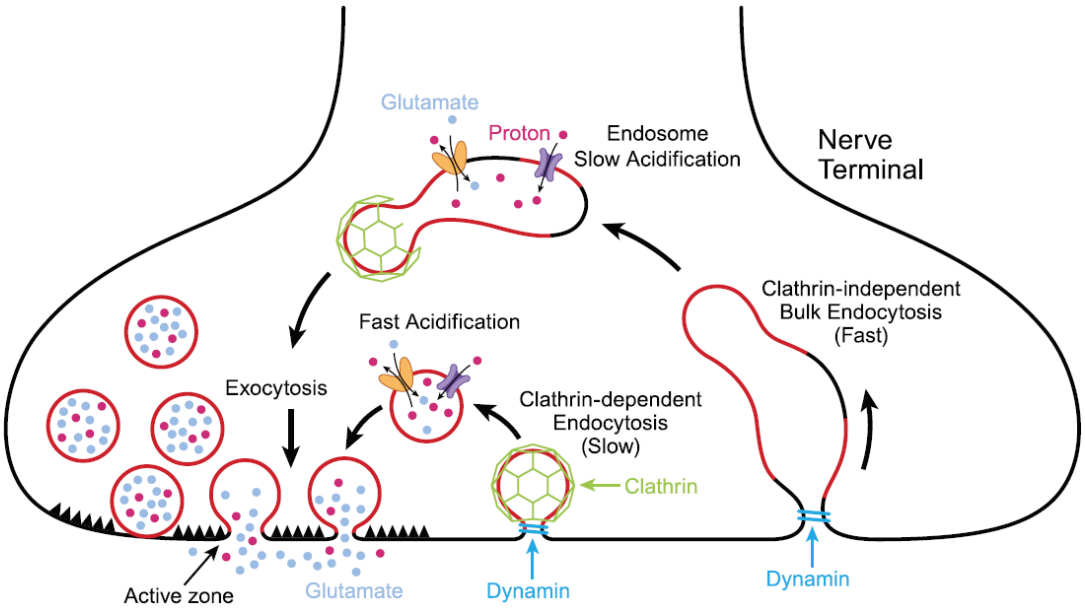

Figure 22. Exo- and endocytosis of membrane and Syt2 at the calyx of Held terminal
SVs fuse with the plasma membrane at the active zones to release neurotransmitter. Fused SV components (membrane and proteins such as Syt2) have to be retrieved by endocytosis, and recycled for reuse. The lumen of SVs is acidic due to proton pumps, which load protons into SVs. Slow endocytosis is mediated by clathrin and dynamin, and these proteins generate new SVs directly from the plasma membrane. Fast endocytosis retrieves large endosome-like structures that slowly become acidic. Both slow and fast endocytosis retrieve membrane and Syt2, and this coordinated retrieval of membrane and Syt2 depend on Ca^{2+}-CaM-Munc13-1 signaling. Image from Gross and von Gersdorff (2016).

4.4. Outlook

I simultaneously monitored the kinetics of SV membrane and vesicular protein (Syt2) retrieval in combination with capacitance measurements and optical imaging of the pH sensitive probe (anti-Syt2-cypHer) at the calyx of Held terminals. To my knowledge, this is the first simultaneous measurements of SV membrane and SV protein retrieval. These findings indicate that the calyx of Held presynaptic terminals have at least two kinetically distinct modes of SV endocytosis, which is consistent with a previous study using photo-conversion of FM dyes at the calyx of Held (Fig 22, de Lange et al., 2003). In addition, my data suggests that Ca^{2+}-CaM-Munc13-1 signaling pathway regulates the retrieval of Syt2 and is likely to be involved in the release site clearance of Syt2 from the AZ.

In the future, I have to investigate:

(1) whether inhibition of Ca^{2+}-CaM-Munc13-1 signaling pathway does cause a traffic jam of SV proteins at the AZs. Although I have seen delayed retrieval of Syt2, which is consistent with delayed clearance of released materials from the release site, more direct demonstration is required. It still remains possible that Ca^{2+}-CaM-Munc13-1 signaling pathway may regulate sorting of SV proteins before endocytosis. To resolve these alternative possibilities, I have to use high resolution microscopy such as STED or STORM microscopy for direct visualization (Hua et al., 2013).

(2) whether decoupling of retrieval between SV membrane and proteins artificially perturbed by CaM inhibition occurs under physiological stimulus conditions or at physiological temperature. Perhaps under intense and/or prolonged stimulation, delayed retrieval of the exocytosed proteins may happen that may have functional consequence such as slowed SV replenishment.

(3) whether Ca^{2+}-CaM-Munc13-1 signaling pathway regulates other SV proteins retrieval, such as synaptobrevin and VGLUT, in the same preparation or Syt2 specifically. For this, I have to introduce optical probes (cypHer or pHluorin) coupled to various SV proteins.

(4) whether Ca^{2+}-CaM-Munc13-1 signaling pathway is involved in the post fusion processes in other types of synapses.

5. References

Adie EJ, Francis MJ, Davies J, Smith L, Marenghi A, Hather C, Hadingham K, Michael NP, Milligan G, Game S. (2003). CypHer 5: a generic approach for measuring the activation and trafficking of G protein-coupled receptors in live cells. *Assay and Drug Development Technologies* **1**:251–259. doi: 10.1089/15406580360545062

Armbruster M, Messa M, Ferguson SM, De Camilli P, Ryan TA. (2013). Dynamin phosphorylation controls optimization of endocytosis for brief action potential bursts. *eLife* **2**:e00845. doi: 10.7554/eLife.00845

Atluri PP, Ryan TA. (2006). The kinetics of synaptic vesicle reacidification at hippocampal nerve terminals. *Journal of Neuroscience* **26**:2313–2320. doi: 10.1523/JNEUROSCI.4425-05.2006

Balaji J, Ryan TA. (2007). Single-vesicle imaging reveals that synaptic vesicle exocytosis and endocytosis are coupled by a single stochastic mode. *Proceedings of the National Academy of Sciences of the United States of America* **104**:20576–20581. doi: 10.1073/pnas.0707574105

Betz A, Okamoto M, Benseler F, Brose N. (1997). Direct interaction of the rat unc-13 homologue Munc13-1 with the N terminus of syntaxin. *The Journal of Biological Chemistry* **272**:2520–2526.

Betz W, Bewick G. (1992). Optical analysis of synaptic vesicle recycling at the frog neuromuscular junction. *Science* **255**:200–203. doi: 10.1126/science.1553547

Brose N, Petrenko AG, Südhof TC, Jahn R. (1992). Synaptotagmin: a calcium sensor on the synaptic vesicle surface. *Science* **256**:1021–1025. doi: 10.1126/science.1589771

Ceccarelli B, Hurlbut WP, Mauro A. (1973). Turnover of transmitter and synaptic vesicles at the frog neuromuscular junction. *The Journal of Cell Biology* **57**:499–524. doi: 10.1083/jcb.57.2.499

Cheung G, Jupp OJ, Cousin MA. (2010). Activity-dependent bulk endocytosis and clathrin-dependent endocytosis replenish specific synaptic vesicle pools in central nerve terminals. *Journal of Neuroscience* **30**:8151–8161. doi: 10.1523/JNEUROSCI.0293-10.2010

Cho S, von Gersdorff H. (2014). Proton-mediated block of Ca^{2+} channels during multivesicular release regulates short-term plasticity at an auditory hair cell synapse. *Journal of Neuroscience* **34**:15877–15887. doi: 10.1523/JNEUROSCI.2304-14.2014

Cremona O, De Camilli P. (1997). Synaptic vesicle endocytosis. *Current Opinion in Neurobiology*

7:323–330. doi: 10.1016/S0959-4388(97)80059-1

de Lange RP, de Roos AD, Borst JG. (2003). Two modes of vesicle recycling in the rat calyx of Held. *Journal of Neuroscience* **23**:10164–10173.

de Wit H, Walter AM, Milosevic I, Gulyás-Kovács A, Riedel D, Sørensen JB, Verhage M. (2009). Synaptotagmin-1 docks secretory vesicles to syntaxin-1/SNAP-25 acceptor complexes. *Cell* **138**:935–46. doi: 10.1016/j.cell.2009.07.027.

Delvendahl I, Jablonski L, Baade C, Matveev V, Neher E, Hallermann S. (2015). Reduced endogenous Ca^{2+} buffering speeds active zone Ca^{2+} signaling. *Proceedings of the National Academy of Sciences of the United States of America* **112**:E3075–3084. doi: 10.1073/pnas.1508419112

Deák F, Schoch S, Liu X, Südhof TC, Kavalali ET. (2004). Synaptobrevin is essential for fast synaptic-vesicle endocytosis. *Nature Cell Biology* **6**:1102–1108. doi: 10.1038/ncb1185

Egashira Y, Takase M, Takamori S. (2015). Monitoring of vacuolar-type H^+ATPase-mediated proton influx into synaptic vesicles. *Journal of Neuroscience* **35**:3701–3710. doi: 10.1523/JNEUROSCI.4160-14.2015

Fernández-Alfonso T, Kwan R, Ryan TA. (2006). Synaptic vesicles interchange their membrane proteins with a large surface reservoir during recycling. *Neuron* **51**:179–186. doi: 10.1016/j.neuron.2006.06.008

Fernández-Alfonso T, Ryan TA. (2004). The kinetics of synaptic vesicle pool depletion at CNS synaptic terminals. *Neuron* **41**:943–953. doi: 10.1016/S0896-6273(04)00113-8

Fesce R, Grohovaz F, Valtorta F, Meldolesi J. (1994). Neurotransmitter release: Fusion or 'kiss-and-run'?. *Trends in Cell Biology* **4**:1–4. doi: 10.1016/0962-8924(94)90025-6

Forsythe ID. (1994). Direct patch recording from identified presynaptic terminals mediating glutamatergic EPSCs in the rat CNS, in vitro. *The Journal of Physiology* **479**:381–387. doi: 10.1113/jphysiol.1994.sp020303

Gandhi SP, Stevens CF. (2003). Three modes of synaptic vesicular recycling revealed by single-vesicle imaging. *Nature* **423**:607–613. doi: 10.1038/nature01677

Geppert M, Goda Y, Hammer RE, Li C, Rosahl TW, Stevens CF, Südhof TC. (1994). Synaptotagmin I: a major Ca^{2+} sensor for transmitter release at a central synapse. *Cell* **79**:717-27. doi: 10.1016/0092-8674(94)90556-8

Granseth B, Odermatt B, Royle SJ, Lagnado L. (2006). Clathrin-mediated endocytosis is the

dominant mechanism of vesicle retrieval at hippocampal synapses. *Neuron* **51**:773–786. doi: 10.1016/j.neuron.2006.08.029

Gross OP, von Gersdorff H. (2016). Recycling at synapses. *eLife* e17692. doi: 10.7554/eLife.17692.

Haucke V, Neher E, Sigrist SJ. (2011). Protein scaffolds in the coupling of synaptic exocytosis and endocytosis. *Nature Reviews Neuroscience* **12**:127–38. doi: 10.1038/nrn2948.

Hallermann S, Pawlu C, Jonas P, Heckmann M. (2003). A large pool of releasable vesicles in a cortical glutamatergic synapse. *Proceedings of the National Academy of Sciences of the United States of America* **100**:8975–8980. doi: 10.1073/pnas.1432836100

Heuser JE, Reese TS. (1973). Evidence for recycling of synaptic vesicle membrane during transmitter release at the frog neuromuscular junction. *The Journal of Cell Biology* **57**:315–344. doi: 10.1083/jcb.57.2.315

Holt M, Cooke A, Wu MM, Lagnado L. (2003). Bulk membrane retrieval in the synaptic terminal of retinal bipolar cells. *Journal of Neuroscience* **23**:1329–1339.

Hori T, Takahashi T. (2012). Kinetics of synaptic vesicle refilling with neurotransmitter glutamate. *Neuron* **76**:511–518. doi: 10.1016/j.neuron.2012.08.013

Hosoi N, Holt M, Sakaba T. (2009). Calcium dependence of exo- and endocytotic coupling at a glutamatergic synapse. *Neuron* **63**:216–229. doi: 10.1016/j.neuron.2009.06.010

Hua Y, Sinha R, Martineau M, Kahms M, Klingauf J. (2010). A common origin of synaptic vesicles undergoing evoked and spontaneous fusion. *Nature Neuroscience* **13**:1451–1453. doi: 10.1038/nn.2695

Hua Y, Sinha R, Thiel CS, Schmidt R, Hüve J, Martens H, Hell SW, Egner A, Klingauf J. (2011). A readily retrievable pool of synaptic vesicles. *Nature Neuroscience* **14**:833–839. doi: 10.1038/nn.2838

Hua Y, Woehler A, Kahms M, Haucke V, Neher E, Klingauf J. (2013). Blocking endocytosis enhances short-term synaptic depression under conditions of normal availability of vesicles. *Neuron* **80**:343–349. doi: 10.1016/j.neuron.2013.08.010

Jahn R, Scheller RH. (2006). SNAREs - engines for membrane fusion. *Nature Reviews Molecular Cell Biology* **7**:631–43. doi:10.1038/nrm2002

Jockusch WJ, Praefcke GJ, McMahon HT, Lagnado L. (2005). Clathrin-dependent and clathrin-independent retrieval of synaptic vesicles in retinal bipolar cells. *Neuron* **46**:869–878. doi: 10.1016/j.neuron.2005.05.004

Junge HJ, Rhee JS, Jahn O, Varoqueaux F, Spiess J, Waxham MN, Rosenmund C, Brose N. (2004). Calmodulin and Munc13 form a Ca^{2+} sensor/effector complex that controls short-term synaptic plasticity. *Cell* **118**:389–401. doi: 10.1016/j.cell.2004.06.029

Kandel ER, Schwartz JH, Jessell TM. (2000). Principles of Neural Science (4th Ed.). *McGraw-Hill*

Kawaguchi SY, Sakaba T. (2015). Control of inhibitory synaptic outputs by low excitability of axon terminals revealed by direct recording. *Neuron* **85**:1273–1288. doi: 10.1016/j.neuron.2015.02.013

Kawasaki F, Hazen M, Ordway RW. (2000). Fast synaptic fatigue in shibire mutants reveals a rapid requirement for dynamin in synaptic vesicle membrane trafficking. *Nature Neuroscience* **3**:859–860. doi: 10.1038/78753

Kononenko NL, Diril MK, Puchkov D, Kintscher M, Koo SJ, Pfuhl G, Winter Y, Wienisch M, Klingauf J, Breustedt J, Schmitz D, Maritzen T, Haucke V. (2013). Compromised fidelity of endocytic synaptic vesicle protein sorting in the absence of stonin 2. *Proceedings of the National Academy of Sciences of the United States of America* **110**:E526–535. doi: 10.1073/pnas.1218432110

Kononenko NL, Haucke V. (2015). Molecular mechanisms of presynaptic membrane retrieval and synaptic vesicle reformation. *Neuron* **85**:484–496. doi: 10.1016/j.neuron.2014.12.016

Kononenko NL, Puchkov D, Classen GA, Walter AM, Pechstein A, Sawade L, Kaempf N, Trimbuch T, Lorenz D, Rosenmund C, Maritzen T, Haucke V. (2014). Clathrin/AP-2 mediate synaptic vesicle reformation from endosome-like vacuoles but are not essential for membrane retrieval at central synapses. *Neuron* **82**:981–988. doi: 10.1016/j.neuron.2014.05.007

Koo SJ, Markovic S, Puchkov D, Mahrenholz CC, Beceren-Braun F, Maritzen T, Dernedde J, Volkmer R, Oschkinat H, Haucke V. (2011). SNARE motif-mediated sorting of synaptobrevin by the endocytic adaptors clathrin assembly lymphoid myeloid leukemia (CALM) and AP180 at synapses. *Proceedings of the National Academy of Sciences of the United States of America* **108**:13540–13545. doi: 10.1073/pnas.1107067108

Lindau M, Neher E. (1988). Patch-clamp techniques for time-resolved capacitance measurements in single cells. *PflüGers Archiv* **411**:137–146. doi: 10.1007/BF00582306

Lipstein N, Sakaba T, Cooper BH, Lin KH, Strenzke N, Ashery U, Rhee JS, Taschenberger H, Neher E, Brose N. (2013). Dynamic control of synaptic vesicle replenishment and short-term plasticity by Ca^{2+}-Calmodulin-Munc13-1 signaling. *Neuron* **79**:82–96. doi: 10.1016/j.neuron.2013.05.011

Lipstein N, Schaks S, Dimova K, Kalkhof S, Ihling C, Kölbel K, Ashery U, Rhee J, Brose N, Sinz A, Jahn O. (2012). Nonconserved Ca^{2+}/calmodulin binding sites in Munc13s differentially control

synaptic short-term plasticity. *Molecular and Cellular Biology* **32**:4628–4641. doi: 10.1128/MCB.00933-12

Ma C, Su L, Seven AB, Xu Y, Rizo J. (2013). Reconstitution of the vital functions of Munc18 and Munc13 in neurotransmitter release. *Science* **339**:421–425. doi: 10.1126/science.1230473

McAdam RL, Varga KT, Jiang Z, Young FB, Blandford V, McPherson PS, Gong LW, Sossin WS. (2015). The juxtamembrane region of synaptotagmin 1 interacts with dynamin 1 and regulates vesicle fission during compensatory endocytosis in endocrine cells. *Journal of Cell Science* **128**:2229–2235. doi: 10.1242/jcs.161505

Midorikawa M, Okamoto Y, Sakaba T. (2014). Developmental changes in Ca^{2+} channel subtypes regulating endocytosis at the calyx of Held. *The Journal of Physiology* **592**:3495–3510. doi: 10.1113/jphysiol.2014.273243

Midorikawa M, Sakaba T. (2015). Imaging exocytosis of single synaptic vesicles at a fast CNS presynaptic terminal. *Neuron* **88**:492–498. doi: 10.1016/j.neuron.2015.09.047

Miesenböck G, De Angelis DA, Rothman JE. (1998). Visualizing secretion and synaptic transmission with pH-sensitive green fluorescent proteins. *Nature* **394**:192–195. doi: 10.1038/28190

Milosevic I, Giovedi S, Lou X, Raimondi A, Collesi C, Shen H, Paradise S, O'Toole E, Ferguson S, Cremona O, De Camilli P. (2011). Recruitment of endophilin to clathrin-coated pit necks is required for efficient vesicle uncoating after fission. *Neuron* **72**:587–601. doi: 10.1016/j.neuron.2011.08.029

Moser T, Beutner D. (2000). Kinetics of exocytosis and endocytosis at the cochlear inner hair cell afferent synapse of the mouse. *Proceedings of the National Academy of Sciences of the United States of America* **97**:883–888. doi: 10.1073/pnas.97.2.883

Neher E. What is rate-limiting during sustained synaptic activity: vesicle supply or the availability of release sites. *Frontiers in Synaptic Neuroscience* **2**:144. doi: 10.3389/fnsyn.2010.00144.

Neher E, Sakaba T. (2008). Multiple roles of calcium ions in the regulation of neurotransmitter release. *Neuron* **59**:861–72. doi: 10.1016/j.neuron.2008.08.019

Nicholson-Tomishima K, Ryan TA. (2004). Kinetic efficiency of endocytosis at mammalian CNS synapses requires synaptotagmin I. *Proceedings of the National Academy of Sciences of the United States of America* **101**:16648–16652. doi: 10.1073/pnas.0406968101

Nicholson-Fish JC, Kokotos AC, Gillingwater TH, Smillie KJ, Cousin MA. (2015). VAMP4 is an essential cargo molecule for activity-dependent bulk endocytosis. *Neuron* **88**:973–984. doi:

10.1016/j.neuron.2015.10.043.

Opazo F, Rizzoli SO. (2010). The fate of synaptic vesicle components upon fusion. *Communicative & Integrative Biology* **3**:427–429. doi: 10.4161/cib.3.5.12132

Pan PY, Marrs J, Ryan TA. (2015). Vesicular glutamate transporter 1 orchestrates recruitment of other synaptic vesicle cargo proteins during synaptic vesicle recycling. *The Journal of Biological Chemistry* **290**:22593–22601. doi: 10.1074/jbc.M115.651711

Pang ZP, Sun J, Rizo J, Maximov A, Südhof TC. (2006). Genetic analysis of synaptotagmin 2 in spontaneous and Ca^{2+}-triggered neurotransmitter release. *The EMBO Journal* **25**:2039–2050. doi: 10.1038/sj.emboj.7601103

Renden R, von Gersdorff H. (2007). Synaptic vesicle endocytosis at a CNS nerve terminal: Faster kinetics at physiological temperatures and increased endocytotic capacity during maturation. *Journal of Neurophysiology* **98**:3349–3359. doi: 10.1152/jn.00898.2007

Rizzoli SO, Betz WJ. (2005). Synaptic vesicle pools. *Nature Reviews Neuroscience* **6:**57–69. doi:10.1038/nrn1583

Sakaba T, Neher E. (2001). Calmodulin mediates rapid recruitment of fast-releasing synaptic vesicles at a calyx-type synapse. *Neuron* **32**:1119–1131. doi: 10.1016/S0896-6273(01)00543-8

Sankaranarayanan S, Ryan TA. (2001). Calcium accelerates endocytosis of vSNAREs at hippocampal synapses. *Nature Neuroscience* **4**:129–136. doi: 10.1038/83949

Schikorski T, Stevens CF. (2001). Morphological correlates of functionally defined synaptic vesicle populations. *Nature Neuroscience* **4**:391–395. doi: 10.1038/86042

Südhof TC. (2004). The synaptic vesicle cycle. *Annual Review of Neuroscience* **27**:509–547. doi: 10.1146/annurev.neuro.26.041002.131412

Südhof TC. (2012). The presynaptic active zone. *Neuron* **75**:11–25. doi: 10.1016/j.neuron.2012.06.012

Sun JY, Wu LG. (2001). Fast kinetics of exocytosis revealed by simultaneous measurements of presynaptic capacitance and postsynaptic currents at a central synapse. *Neuron* **30**:171–182. doi: 10.1016/S0896-6273(01)00271-9

Sun T, Wu XS, Xu J, McNeil BD, Pang ZP, Yang W, Bai L, Qadri S, Molkentin JD, Yue DT, Wu LG. (2010). The role of calcium/calmodulin-activated calcineurin in rapid and slow endocytosis at central synapses. *Journal of Neuroscience* **30**:11838–11847. doi: 10.1523/JNEUROSCI.1481-10.2010

Sätzler K, Söhl LF, Bollmann JH, Borst JG, Frotscher M, Sakmann B, Lübke JH. (2002). Three-dimensional reconstruction of a calyx of Held and its postsynaptic principal neuron in the medial nucleus of the trapezoid body. *Journal of Neuroscience* **22**:10567–10579.

Takei K, Haucke V, Slepnev V, Farsad K, Salazar M, Chen H, De Camilli P. (1998). Generation of coated intermediates of clathrin-mediated endocytosis on protein-free liposomes. *Cell* **94**:131–141. doi: 10.1016/S0092-8674(00)81228-3

Takamori S, Rhee JS, Rosenmund C, Jahn R. (2000). Identification of a vesicular glutamate transporter that defines a glutamatergic phenotype in neurons. *Nature* **407**:189–94. doi: 10.1038/35025070

Taschenberger H, Leão RM, Rowland KC, Spirou GA, von Gersdorff H. (2002). Optimizing synaptic architecture and efficiency for high-frequency transmission. *Neuron* **36**:1127–1143. doi: 10.1016/S0896-6273(02)01137-6

Thomas P, Lee AK, Wong JG, Almers W. (1994). A triggered mechanism retrieves membrane in seconds after Ca^{2+}-stimulated exocytosis in single pituitary cells. *The Journal of Cell Biology* **124**:667–675. doi: 10.1083/jcb.124.5.667

Traub LM. (2009). Tickets to ride: Selecting cargo for clathrin-regulated internalization. *Nature Reviews Molecular Cell Biology* **10**:583–596. doi: 10.1038/nrm2751

Varoqueaux F, Sigler A, Rhee JS, Brose N, Enk C, Reim K, Rosenmund C. (2002). Total arrest of spontaneous and evoked synaptic transmission but normal synaptogenesis in the absence of Munc13-mediated vesicle priming. *Proceedings of the National Academy of Sciences of the United States of America* **99**:9037–9042. doi: 10.1073/pnas.122623799

von Gersdorff H, Mathews G. (1994). Dynamics of synaptic vesicle fusion and membrane retrieval in synaptic terminals. *Nature* **367**:735–739. doi: 10.1038/367735a0

Watanabe S, Rost BR, Camacho-Pérez M, Davis MW, Söhl-Kielczynski B, Rosenmund C, Jorgensen EM. (2013). Ultrafast endocytosis at mouse hippocampal synapses. *Nature* **504**:242–247. doi: 10.1038/nature12809

Watanabe S, Trimbuch T, Camacho-Pérez M, Rost BR, Brokowski B, Söhl-Kielczynski B, Felies A, Davis MW, Rosenmund C, Jorgensen EM. (2014). Clathrin regenerates synaptic vesicles from endosomes. *Nature* **515**:228–233. doi: 10.1038/nature13846

Wienisch M, Klingauf J. (2006). Vesicular proteins exocytosed and subsequently retrieved by compensatory endocytosis are nonidentical. *Nature Neuroscience* **9**:1019–1027. doi: 10.1038/nn1739

Wu LG, Borst JG. (1999). The reduced release probability of releasable vesicles during recovery from short-term synaptic depression. *Neuron* **23**:821–832. doi: 10.1016/S0896-6273(01)80039-8

Wu LG, Ryan TA, Lagnado L. (2007). Modes of vesicle retrieval at ribbon synapses, calyx-type synapses, and small central synapses. *Journal of Neuroscience* **27**:11793–802.

Wu W, Xu J, Wu XS, Wu LG. (2005). Activity-dependent acceleration of endocytosis at a central synapse. *Journal of Neuroscience* **25**:11676–11683. doi: 10.1523/JNEUROSCI.2972-05.2005

Wu XS, McNeil BD, Xu J, Fan J, Xue L, Melicoff E, Adachi R, Bai L, Wu LG. (2009). Ca^{2+} and calmodulin initiate all forms of endocytosis during depolarization at a nerve terminal. *Nature Neuroscience* **12**:1003–1010. doi: 10.1038/nn.2355

Wu XS, Zhang Z, Zhao WD, Wang D, Luo F, Wu LG. (2014). Calcineurin is universally involved in vesicle endocytosis at neuronal and nonneuronal secretory cells. *Cell Reports* **7**:982–988. doi: 10.1016/j.celrep.2014.04.020

Xu J, McNeil B, Wu W, Nees D, Bai L, Wu LG. (2008). GTP-independent rapid and slow endocytosis at a central synapse. *Nature Neuroscience* **11**:45–53. doi: 10.1038/nn2021

Xu J, Mashimo T, Südhof TC. (2007). Synaptotagmin-1, -2, and -9: Ca^{2+} sensors for fast release that specify distinct presynaptic properties in subsets of neurons. *Neuron* **54**:567–81. doi: 10.1016/j.neuron.2007.05.004

Xue L, McNeil BD, Wu XS, Luo F, He L, Wu LG. (2012). A membrane pool retrieved via endocytosis overshoot at nerve terminals: A study of its retrieval mechanism and role. *Journal of Neuroscience* **32**:3398–3404. doi: 10.1523/JNEUROSCI.5943-11.2012

Yamashita T. (2012). Ca^{2+}-dependent regulation of synaptic vesicle endocytosis. *Neuroscience Research* **73**:1–7. doi: 10.1016/j.neures.2012.02.012

Yamashita T, Eguchi K, Saitoh N, von Gersdorff H, Takahashi T. (2010). Developmental shift to a mechanism of synaptic vesicle endocytosis requiring nanodomain Ca^{2+}. *Nature Neuroscience* **13**:838–844. doi: 10.1038/nn.2576

Yamashita T, Hige T, Takahashi T. (2005). Vesicle endocytosis requires dynamin-dependent GTP hydrolysis at a fast CNS synapse. *Science* **307**:124–127. doi: 10.1126/science.1103631

Yao J, Nowack A, Kensel-Hammes P, Gardner RG, Bajjalieh SM. (2010). Cotrafficking of SV2 and synaptotagmin at the synapse. *Journal of Neuroscience* **30**:5569–5578. doi: 10.1523/JNEUROSCI.4781-09.2010

Yao L, Sakaba T. (2012). Activity-dependent modulation of endocytosis by calmodulin at a large central synapse. *Proceedings of the National Academy of Sciences of the United States of America* **109**:291–296. doi: 10.1073/pnas.1100608109

Yao LH, Rao Y, Varga K, Wang CY, Xiao P, Lindau M, Gong LW. (2012). Synaptotagmin 1 is necessary for the Ca^{2+} dependence of clathrin-mediated endocytosis. *Journal of Neuroscience* **32**:3778–3785. doi: 10.1523/JNEUROSCI.3540-11.2012

Zhang Z, Wang D, Sun T, Xu J, Chiang HC, Shin W, Wu LG. (2013). The SNARE proteins SNAP25 and synaptobrevin are involved in endocytosis at hippocampal synapses. *Journal of Neuroscience* **33**:9169–9175. doi: 10.1523/JNEUROSCI.0301-13.2013

Zhou Q, Lai Y, Bacaj T, Zhao M, Lyubimov AY, Uervirojnangkoorn M, Zeldin OB, Brewster AS, Sauter NK, Cohen AE, Soltis SM, Alonso-Mori R, Chollet M, Lemke HT, Pfuetzner RA, Choi UB, Weis WI, Diao J, Südhof TC, Brunger AT. (2015). Architecture of the synaptotagmin-SNARE machinery for neuronal exocytosis. *Nature* **525**:62–7. doi: 10.1038/nature14975.